and on the induction of a yolk precursor in goldfish, *Carassius auratus*. Life Sci. 20, 1945–1952.

Edman, P., 1956. On the mechanism of the isothiocyanate degradation of peptides. Acta Chem. Scand. 10, 761–768.

Falchuk, K.H., Montorzi, M., 2001. Zinc physiology and biochemistry in oocytes and embryos. BioMetals 14, 385–395.

Fisher, C.L., Cabelli, D.E., Tainer, J.A., Hallewell, R.A., Getzoff, E.D., 1994. The role of arginine 143 in the electrostatics and mechanism of Cu,Zn superoxide dismutase: computational and experimental evaluation by mutational analysis. Proteins 19, 24–34.

Gronen, S., Denslow, N., Manning, S., Barnes, S., Barnes, D., Brouwer, M., 1999. Serum vitellogenin levels and reproductive impairment of male Japanese medaka (*Oryzias latipes*) exposed to 4-*tert*-octylphenol. Environ. Health Perspect. 107, 385–390.

Hegyi, H., Bork, P., 1997. On the classification and evolution of protein modules. J. Protein Chem. 16, 545–551.

Kato, K., Tokishita, S., Mandokoro, Y., Kimura, S., Ohta, T., Kobayashi, M., Yamagata, H., 2001. Two-domain hemoglobin gene of the water flea *Moina macrocopa*: duplication in the ancestral cladocera, diversification, and loss of a bridge intron. Gene 273, 41–50.

Kijimoto-Ochiai, S., Katagiri, Y.U., Ochiai, H., 1985. Analysis of N-linked oligosaccharide chains of glycoproteins on nitrocellulose sheets using lectin-peroxidase reagents. Anal. Biochem. 147, 222–229.

Kimura, S., Tokishita, S., Ohta, T., Kobayashi, M., Yamagata, H., 1999. Heterogeneity and differential expression under hypoxia of two-domain hemoglobin chains in the water flea *Daphnia magna*. J. Biol. Chem. 274, 10649–10653.

Laemmli, U.K., 1970. Cleavage of structural proteins during the assembly of the head of bacteriophage T4. Nature 227, 680–685.

Li, A., Sadasivam, M., Ding, J.L., 2002. Receptor-ligand interaction between vitellogenin receptor (VtgR) and vitellogenin (Vtg), implications on low density lipoprotein receptor and apolipoprotein B/E. The first three ligand-binding repeats of VtgR interact with the amino-terminal region of Vtg. J. Biol. Chem. 278, 2799–2806.

Mann, C.J., Anderson, T.A., Read, J., Chester, S.A., Harrison, G.B., Kochl, S., Ritche, P.J., Bradbury, P., Hussain, F.S., Amey, J., Vanloo, B., Rosseneu, M., Infante, R., Hancock, J.M., Levitt, D.G., Banaszak, L.J., Scott, J., Shoulders, C.C., 1999. The structure of vitellogenin provides a molecular model for the assembly and secretion of atherogenic lipoproteins. J. Mol. Biol. 285, 391–408.

McLachlan, J.A., Arnold, S.E., 1996. Environmental estrogens. Am. Sci. 84, 452–461.

Montesano, L., Carri, M.T., Mariottini, P., Amaldi, F., Rotillo, G., 1989. Developmental expression of Cu,Zn superoxide dismutase in *Xenopus*. Constant level of the enzyme in oogenesis and embryogenesis. Eur. J. Biochem. 186, 421–426.

Peretz-Vilar, J., Hill, R.H., 1998. Identification of the half-cystine residues in porcine submaxillary mucin critical for multimerization through the D-domains. Roles of the CGLCG motif in the D1- and D3-domains. J. Biol. Chem. 273, 34527–34534.

Raikhel, A.S., Dhadialla, T.S., 1992. Accumulation of yolk proteins in insect oocytes. Annu. Rev. Entomol. 37, 217–251.

Sappington, T.W., Raikhel, A.S., 1998. Molecular characteristics of insect vitellogenins and vitellogenin receptors. Insect Biochem. Mol. Biol. 28, 277–300.

Seidah, N.G., Prat, A., 2002. Precursor convertases in the secretory pathway, cytosol and extracellular milieu. Essays Biochem. 38, 79–94.

Shoulders, C.C., Narcisi, T.M., Read, J., Chester, A., Brett, D.J., Scott, J., Anderson, T.A., Levitt, D.G., Banaszak, L.J., 1994. The abetalipoproteinemia gene is a member of the vitellogenin family and encodes an alpha-helical domain. Nat. Struct. Biol. 1, 285–286.

Thompson, J.D., Gibson, T.J., Plewniak, F., Jeanmougin, F., Higgins, D.G., 1997. The CLUSTAL_X windows interface: flexible strategies for multiple sequence alignment aided by quality analysis tools. Nucleic Acids Res. 25, 4876–4882.

Tokishita, S., Shiga, Y., Kimura, S., Ohta, T., Kobayashi, M., Hanazato, T., Yamagata, H., 1997. Cloning and analysis of a cDNA encoding a two-domain hemoglobin chain from the water flea *Daphnia magna*. Gene 189, 73–78.

Von Heijne, G., 1986. A new method for predicting signal sequence cleavage sites. Nucleic Acids Res. 14, 4683–4690.

Published online 22 July 2004

Nucleic Acids Research, 2004, Vol. 32, No. 13 ***e109***
doi:10.1093/nar/gnh093

Atelocollagen-mediated synthetic small interfering RNA delivery for effective gene silencing *in vitro* and *in vivo*

Yoshiko Minakuchi, Fumitaka Takeshita[1], Nobuyoshi Kosaka[2], Hideo Sasaki[1], Yusuke Yamamoto[2], Makiko Kouno[3], Kimi Honma[3], Shunji Nagahara, Koji Hanai, Akihiko Sano, Takashi Kato[2], Masaaki Terada[1] and Takahiro Ochiya[1,*]

Formulation Research Laboratories, Sumitomo Pharmaceuticals Co. Ltd, Osaka 567-0878, Japan, [1]National Cancer Center Research Institute, 1-1, Tsukiji 5-chome, Chuo-ku, Tokyo 104-0045, Japan, [2]Department of Biology, School of Education, Waseda University, Tokyo 169-0051, Japan and [3]Koken Bioscience Institute, Tokyo 115-0051, Japan

Received April 8, 2004; Revised May 26, 2004; Accepted June 7, 2004

ABSTRACT

Silencing gene expression by siRNAs is rapidly becoming a powerful tool for the genetic analysis of mammalian cells. However, the rapid degradation of siRNA and the limited duration of its action call for an efficient delivery technology. Accordingly, we describe here that Atelocollagen complexed with siRNA is resistant to nucleases and is efficiently transduced into cells, thereby allowing long-term gene silencing. Site-specific *in vivo* administration of an anti-luciferase siRNA/Atelocollagen complex reduced luciferase expression in a xenografted tumor. Furthermore, Atelocollagen-mediated transfer of siRNA *in vivo* showed efficient inhibition of tumor growth in an orthotopic xenograft model of a human non-seminomatous germ cell tumor. Thus, for clinical applications of siRNA, an Atelocollagen-based non-viral delivery method could be a reliable approach to achieve maximal function of siRNA *in vivo*.

INTRODUCTION

RNA interference (RNAi) as a protecting mechanism against invasion of foreign genes was first described in *Caenorhabditis elegans* (1) and has subsequently been demonstrated in diverse eukaryotes, such as insects, plants, fungi and vertebrates (2). In many eukaryotes, expression of nuclear-encoded mRNA can be strongly inhibited by the presence of a double-stranded RNA (dsRNA) corresponding to exon sequences in the mRNA. RNAi can be exploited in cultured mammalian cells by introducing shorter, synthetic duplex RNAs (~20 nt) through liposome transfection (3–5) and a peptide-based delivery (6). In mammalian cells, siRNAs have become a new and powerful alternative to other genetic knockdown methods for the analysis of loss-of-function phenotypes. In theory, the technique is simple and elegant. In practice, however, limited stability *in vivo* and the absence of a reliable delivery method hamper the utility of siRNA for therapeutic application. Reports have shown that liposomes (7,8), adenovirus (9), adeno-associated viral vectors (10) and lentivirus (11) can be considered as useful delivery systems. A virus vector-based siRNA delivery overcomes the problem of poor transfection efficiency of plasmid-based systems. However, viral vectors have several limitations when they are used *in vivo*.

Atelocollagen is a highly purified pepsin-treated type I collagen from calf dermis. Collagen is a fibrous protein in the connective tissue that plays an important role in the maintenance of the morphology of tissues and organs. A collagen molecule has an amino acid sequence called as telopeptide at both N- and C-terminals, which confers most of the collagen's antigenicity. Atelocollagen obtained by pepsin treatment is low in immunogenicity because it is free from telopeptides (12), and it is used clinically for a wide range of purposes, including wound-healing, vessel prosthesis and also as a bone cartilage substitute and hemostatic agent (13). We have demonstrated previously that Atelocollagen complexed with DNA molecules was efficiently transduced into mammalian cells (14) and allowed long-term gene expression (15). Since Atelocollagen allows increased cellular uptake, nuclease resistance and prolonged release of genes and oligonucleotides (13), an Atelocollagen complex is applicable for an efficient delivery of siRNA *in vitro*. Furthermore, Atelocollagen displays low-toxicity and low-immunogenicity when it is transplanted *in vivo* (13,16). Thus, our gene delivery method using an Atelocollagen implant should permit safe and efficient siRNA-mediated gene silencing in therapeutic applications.

MATERIALS AND METHODS

Atelocollagen

Atelocollagen is a highly purified type I collagen of calf dermis with pepsin treatment (Koken Co., Ltd, Tokyo, Japan).

*To whom correspondence should be addressed. Tel: +81 3 3542 2511; Fax: +81 3 3541 2685; Email: tochiya@ncc.go.jp

siRNA preparation

Synthetic 21-nt RNAs were purchased from Dharmacon (Lafayette, CO) in deprotected, desalted and annealed form. The sequence of our prepared human fibroblast growth factor (FGF)-4 (HST-1/FGF-4) siRNA was 5′-CGAUGAGUGCACGUUCAAGdTdT-3′; 3′-dTdTGCUACUCACGUGCAAGUUC-5′. Non-specific control siRNA duplex (VIII), luciferase GL3 siRNA duplex and luciferase GL2 siRNA were also purchased from Dharmacon, and were used as controls.

Formation of siRNA/Atelocollagen complex

The siRNAs and Atelocollagen complexes were prepared as follows. An equal volume of Atelocollagen (in PBS at pH 7.4) and siRNAs solution was combined and mixed by rotation at 4°C for 20 min. The complex was then kept at 4°C for 16 h before use. The final concentration of Atelocollagen *in vitro* and *in vivo* was 0.008 and 0.5%, respectively.

Stability of siRNA/Atelocollagen complex

An aliquot of 0.9 μg of siRNAs (luciferase GL3 duplex) and 0.5% Atelocollagen or cationic liposome (jetSI; Polyplus-transfection SAS, Illkirch Cedex, France) complexes were incubated in the presence of 0.1 μg/μl RNase A (NipponGene, Tokyo, Japan) for 0, 5, 15, 30, 45 and 60 min at 37°C. The solutions were extracted with phenol and phenol/chloroform/isoamyl alcohol (25:24:1). The siRNAs were precipitated with ethanol and agarose gel electrophoresed (3.5%) and visualized by ethidium bromide staining.

Cell lines

NEC8 cells (American Type Culture Collection, Rockville, MD) derived from human testicular tumor were maintained in DMEM with 10% heat-inactivated FBS at 37°C in a humidified atmosphere of 5% CO_2. Increased expression of the *HST-1/FGF-4* gene in this cell line has been reported previously (17). B16-F10 melanoma cells continuously express luciferase (B16-F10-luc-G5; Xenogen Corp., Alameda, CA) and were maintained in DMEM with 10% heat-inactivated FBS at 37°C in a humidified atmosphere of 5% CO_2.

Atelocollagen or liposome-mediated siRNA transfer

The siRNA/Atelocollagen (0.008%) complexes were prefixed to a 24-well plate (0.1–1.4 μg siRNA/50 μl/well) according to the method described previously (14). The cultured cells were plated into the complex-prefixed 24-well plate at 3.5×10^4 cells/well and the effects of siRNA transfer were then observed. The cationic liposome-mediated transfer of siRNA was performed as described by the manufacturer.

Inhibition of cell growth

For monitoring the inhibition of cell growth, the TetraColor One cell proliferation assay reagent (Seikagaku Co., Tokyo, Japan) was used according to the recommended method. The color reaction was assessed by measuring the absorbance at 450 nm with an UVmicroplate reader.

Biochemical analysis

Protein levels of human HST-1/FGF-4 in the culture supernatant and tumors were determined by using enzyme-linked immunosorbent assay (ELISA) using anti-human FGF-4 monoclonal antibody (R&D Systems, Minneapolis, MN). Absorbance was measured at a wavelength of 492 nm with a kinetic microplate reader (model 3550; Biorad, Richmond, CA).

Luciferase assays

For luciferase-based reporter gene assays, 24 μg pGL3 control vector (Promega, Madison, WI) was introduced into HEK 293 cells at 90% confluency in 10 cm dishes using Lipofect-tAMINE™ 2000 reagent (Invitrogen, Carlsbad, CA) in accordance with the manufacturer's instructions. After transfection for 4 h, the cells were collected by trypsinization and plated in the 24-well dishes for siRNA transfection. Atelocollagen-mediated or conventional transfection of siRNAs into 293 cells was performed as detailed above. Cells were lysed (n = 4) on day 2 and analyzed for luciferase activity (Bright™-Glo Luciferase Assay System; Promega). Inhibition of luciferase production was normalized to the level of vehicle-treated cells. GL2 siRNA was used as control.

Analysis of siRNA delivery using *in vivo* imaging

B16-F10-luc-G5 cells were subcutaneously injected (1×10^5 cells per site) into athymic nude mice. Two days later, luciferase GL3 siRNA alone, siRNA mixed with liposome, siRNA complexed with Atelocollagen and Atelocollagen alone were injected into the tumors. For preparing the siRNA/Atelocollagen complex, an equal volume of Atelocollagen (1.0% in PBS at pH 7.4) and siRNA solution was combined and mixed by rotating for 20 min at 4°C. The siRNAs and their complexes were directly injected into the tumor (2.5 μg siRNA/50 μl/50 mm^3 tumor). The final concentration of Atelocollagen was 0.5%. The siRNA concentration used in the liposome experiments was 2.5 μg/tumor equivalent to that used in the Atelocollagen experiments. Each group contains four animals. *In vivo* bioimaging was conducted on a cryogenically cooled IVIS system (Xenogen Corp.) using LivingImage acquisition and analysis software (18). Tumor growth was not affected by these treatments. As a control for GL3 siRNA, GL2 siRNA was used.

Reporter gene labeling of tumor cells

NEC8 cells were transfected with a complex of 2 μg pEGF-PLuc plasmid DNA (Clontech, Palo Alto, CA) and 30 μl lipofection reagent (LipofectAMINE™ 2000; Invitrogen). Stable transfectants were selected in geneticin (400 μg/ml; Invitrogen) and bioluminescence was used to screen transfected clones for luciferase gene expression using the IVIS system. Clones expressing the luciferase gene were named NEC8-luc.

In vivo imaging study for orthotopic xenografts model

A total of 1.0×10^6 NEC8-luc cells were injected into mice intratesticularly. Cells were suspended in 50 μl of a serum-free medium and injected using a 26-gauge needle into both testes of 8-week-old athymic nude mice obtained from CLEA Japan (Shizuoka, Japan). Ten days after the injection of cells, tumor cell-bearing nude mice were randomly divided into four treatment groups (FGF-4 siRNA alone, FGF-4 siRNA complexed with Atelocollagen, control siRNA complexed with Atelocollagen and Atelocollagen alone). Each group consisted of four animals. The siRNAs and their complexes were injected directly into the testes (2.5 μg siRNA/50 μl/testis). The final

concentration of Atelocollagen was 0.5%. Tumor growth was monitored by measuring light emission from individual mice 21 days after siRNA administration. Three days after siRNA administration, tumors were harvested and subjected to ELISA analysis for the detection of FGF-4 protein. Animal experiments in the present study were performed in compliance with the guidelines of the Institute for Laboratory Animal Research, National Cancer Center Research Institute.

Statistical analysis

The results are given as means ± SE. Statistical analysis was conducted using the analysis of variance with the Bonferroni correction for multiple comparisons. A *P*-value of 0.05 or less was considered to indicate a significant difference.

RESULTS

Atelocollagen-based delivery of siRNA into cells

To develop a method for more efficient siRNA delivery into cells, we have developed a new method for condensing and delivering siRNA using Atelocollagen. Atelocollagen, which is positively charged interacts with the negatively charged siRNA duplex to form an siRNA/Atelocollagen complex (Figure 1),

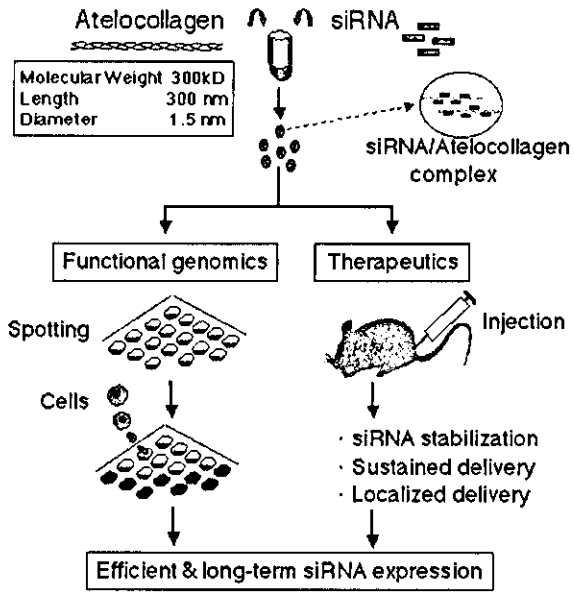

Figure 1. Schematic representation of Atelcollagen-mediated transfer of siRNA duplex for functional genomics and therapeutics. Atelocollagen is a decomposition product of type I collagen derived from the dermis of cattle with a molecular weight of 300 kDa. It is a rod-like molecule with a length and diameter of 300 and 1.5 nm, respectively. Atelocollagen, which is positively charged interacts with the negatively charged siRNA duplex to form an siRNA/Atelocollagen complex, a nanosize particle with a diameter of 100–300 nm. The siRNA/Atelocollagen complex spotted onto the well of a microplate was stable for a long period and allowed the cells to transduce and express siRNAs. The present method using Atelocollagen-based siRNA transfer is also applicable to *in vivo* siRNA transfer, since the siRNA/Atelocollagen complex is stable *in vivo*. Atelocollagen is soluble at a lower temperature but solidifies to refibrillation at a temparature over 30°C. Therefore, the siRNA/Atelocollagen complexes can be injected locally for tissue-targeting siRNA delivery. Once introduced into animals, the complex becomes a solid state and the siRNA is controlled-released for a defined period due to the biodegradable nature of Atelocollagen.

a nanosize particle with a diameter of 100–300 nm. In this system, the siRNA/Atelocollagen complexes are pre-coated on a micro-well plate on which the cells are then seeded (16) (Figure 1). Using this method, cells take up the siRNA/Atelocollagen complex and siRNA exerts a gene silencing effect. To examine whether Atelocollagen blocks degradation of siRNA from nuclease, naked siRNA, siRNA/liposome complex and siRNA/Atelocollagen complex were incubated in the presence of RNase (0.1 μg/μl) for 0, 5, 15, 30, 45 and 60 min at 37°C followed by agarose gel electrophoresis. The results indicated that the siRNA/Atelocollagen complex showed partial resistance to degradation of siRNA in the presence of nuclease (Figure 2). In addition, ~50% of the siRNA were incorporated into the Atelocollagen, which suggests non-incorporated siRNAs are degraded (data not shown). Furthermore, Atelocollagen demonstrated 40–60% efficiency of cellular uptake of FITC-labeled siRNAs 24 h after transfection (data not shown). To evaluate the efficiency of Atelocollagen-mediated transfer technology using well-characterized siRNA, we employed a luciferase reporter

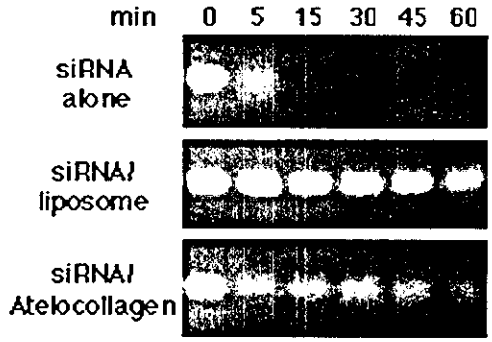

Figure 2. Atelocollagen blocks degradation of siRNA by RNase A. Naked siRNA, siRNA/liposome and siRNA/Atelocollagen complexes were incubated in the presence of RNase A for 0, 5, 15, 30, 45 and 60 min at 37°C and then agarose gel electrophoresed. The presence of siRNA was revealed by ethidium bromide staining.

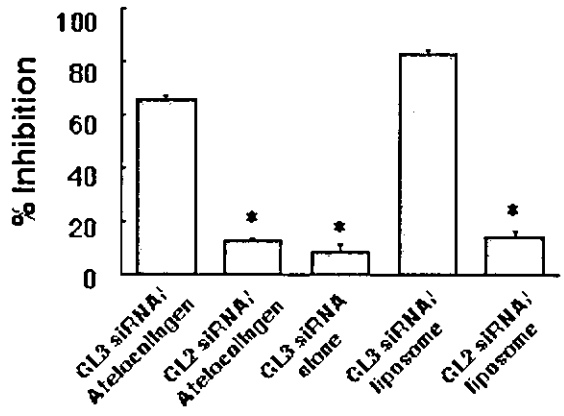

Figure 3. Characteristics of Atelocollagen-mediated siRNA transfer technology. Inhibitory effect of luciferase production in 293 cells. The GL3 siRNA duplexes were transfected into pGL3 control plasmid transfected 293 cells by polycation-reagent or complexed with Atelocollagen. Luciferase activity was measured on day 2 ($n = 4$, mean ± SE). *, $P < 0.001$ versus GL3 siRNA/Atelocollagen and GL3 siRNA liposome-treated cells. As a control for GL3 siRNA, GL2 siRNA was used.

gene system in 293 cells. As shown in Figure 3, our Atelocollagen-mediated siRNA delivery technology exhibited an inhibitory effect as efficient as that in the conventional liposome transfer method.

In the next experiment, we employed human testicular tumor cells, NEC8, which showed high levels of HST-1/FGF-4 mRNA expression (17) and specifically inhibited cell growth by suppression of HST-1/FGF-4 (19). An Atelocollagen-mediated delivery of human HST-1/FGF-4 siRNA was performed to inhibit NEC8 cell growth. The inhibitory effect of HST-1/FGF-4 siRNA was dose-dependent and 1.4 μg per 3.5×10^4 cells produced maximum inhibition (Figure 4A). At a dose of 1.4 μg per 3.5×10^4 cells showed ~10% toxicity by the trypan blue exclusion. Therefore, we used human HST-1/FGF-4 siRNA at a submaximal dose of 0.7 μg per 3.5×10^4 NEC8 cells for further studies. The NEC8 cells transfected with siRNA plus polycation reagent showed an inhibitory effect for maximum of 4 days post-transfection and there was no inhibition of cell growth thereafter (Figure 4B). In addition, siRNA alone and liposome alone showed no significant inhibitory effect (data not shown). In contrast, HST-1/FGF-4 siRNA complexed with Atelocollagen displayed inhibition of cell growth for at least 7 days in culture. To verify further that cell growth inhibition reflected a gene-specific silencing event, HST-1/FGF-4 protein production in NEC8 cells was investigated by ELISA (20). As shown in Figure 5, HST-1/FGF-4 protein levels were significantly inhibited when cells were transfected with the siRNA/Atelocollagen complex. Taken together, these data show that the Atelocollagen stabilized siRNA and thereby siRNA/Atelocollagen complex was able to produce an efficient and a long-term gene silencing effect *in vitro*.

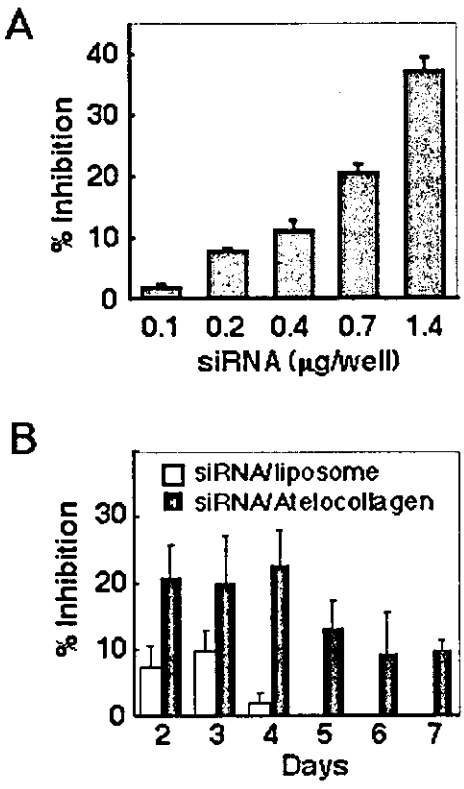

Figure 4. Inhibition of human testicular tumor cell growth by siRNA/Atelocollagen complex. (**A**) Dose-dependent inhibition of NEC8 cell growth. Human HST-1/FGF-4 siRNAs (0.1–1.4 μg) complexed with 0.008% Atelocollagen were transduced into NEC8 cells. Cell proliferation was measured at 2 days after treatment ($n = 4$, mean ± SE). (**B**) Long-term inhibition of NEC8 cell growth by siRNA/Atelocollagen complex. HST-1/FGF-4 siRNA (0.7 μg) was transfected into NEC8 cells by polycation-reagent and complexed with 0.008% Atelocollagen ($n = 6$, mean ± SE).

Enhanced gene silencing by siRNA/Atelocollagen complex *in vivo*

To test whether Atelocollagen-mediated siRNA transfer is valid for gene silencing *in vivo* (Figure 1), animal experiments were performed on mice bearing a luciferase-producing melanoma. Non-invasive *in vivo* bioluminescence imaging analysis showed that luciferase expressions in the tumor of mice injected with GL3 siRNA alone and liposome-complexed siRNA were maximally inhibited at 2–3 days after injection, and increased thereafter. In contrast, mice administered with the siRNA/Atelocollagen complex showed a relatively strong and sustained inhibition of luciferase expression *in vivo* (Figures 6A and B). As previously shown, radiolabeled siRNA mixed with Atelocollagen existed in the tumors for at least a week and remained intact (21). These results suggest that an Atelocollagen-mediated *in vivo* transfer of siRNA could be a powerful and simple method to study loss-of-function of genes in animals.

Inhibition of tumor growth by siRNA/Atelocollagen complex

Testicular injections of NEC8 cell lines in Balb/c nude mice demonstrated relevant tumor biology (19). In this study, the NEC8 cell line was labeled through expression of a stable integrant of the luciferase gene. Athymic nude mice laden

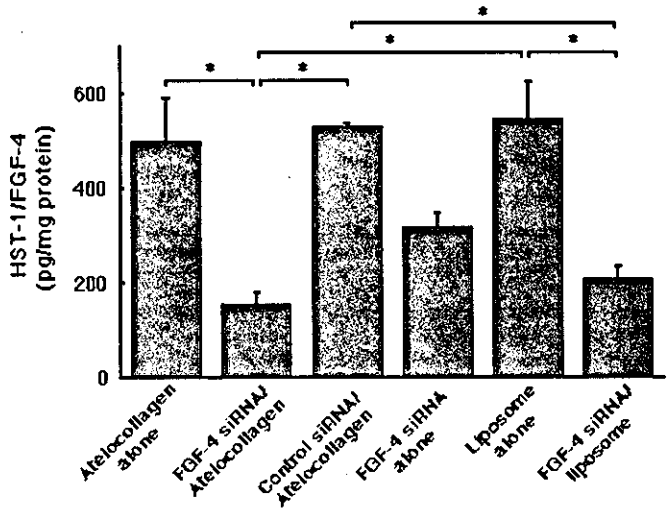

Figure 5. Silencing effect on HST-1/FGF-4 protein production in NEC8 cells. HST-1/FGF-4 siRNA (0.7 μg) complexed with 0.008% Atelocollagen was transduced into NEC8 cells. As a control, an Atelocollagen complex with non-specific control siRNA duplex that shows no silencing effect on human HST-1/FGF-4 was used (control-siRNA/Atelocollagen). Production of HST-1/FGF-4 protein was measured by ELISA 3 days after the transfer of siRNA ($n = 3$, mean ± SE). *, $P < 0.05$.

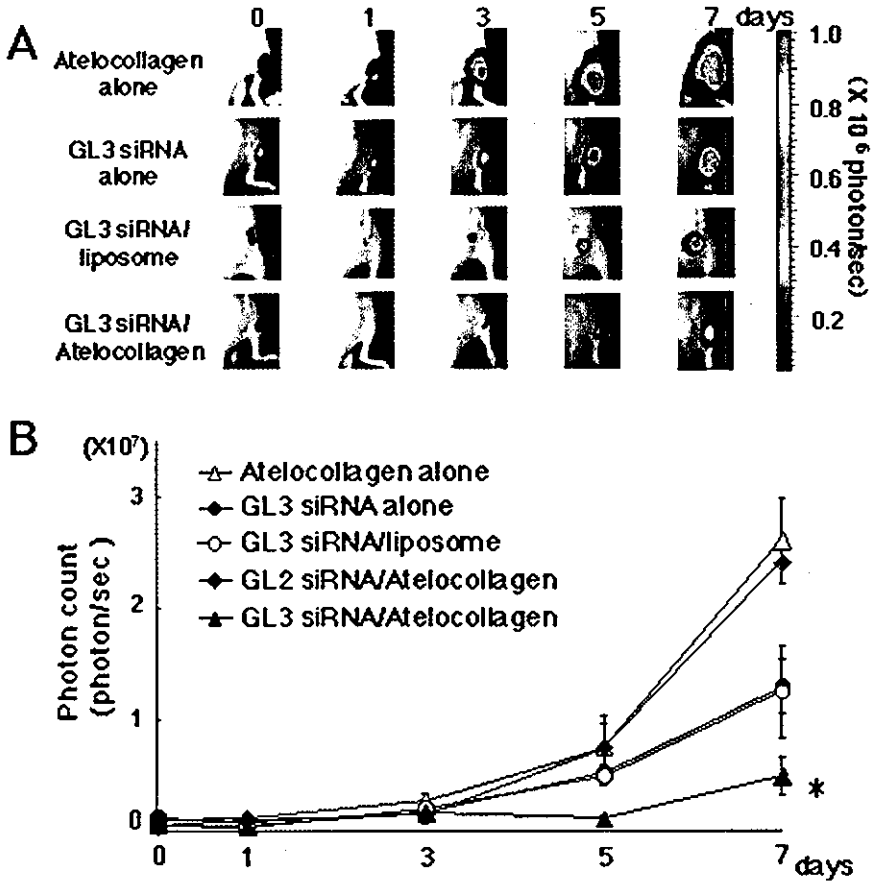

Figure 6. *In vivo* imaging of gene silencing effect of siRNA/Atelocollagen complex. (**A**) Luciferase GL3 siRNA (2.5 μg) complexed with 0.5% Atelocollagen was administered into mice and luciferase expression of xenografted tumors was monitored by *in vivo* imaging analysis. As a control, mice administered with siRNA alone, siRNA complexed with liposome and Atelocollagen alone were investigated. Color bar represents signal intensity code over body surface area. (**B**) Luciferase gene expression was measured periodically and is represented as photon/s. Number of tumors at each time point is 4. As a control for GL3 siRNA, GL2 siRNA was used. Data represent the mean ± SE. *, $P < 0.05$ versus Atelocollagen treatment.

with a testicular injection of NEC8-luc cells were randomly selected for treatment with HST-1/FGF-4 siRNA alone, siRNA complexed with Atelocollagen or Atelocollagen alone. Previously, bioluminescence imaging of orthotopic xenografts in mice demonstrated a linear correlation between tumor bioluminescence and tumor volume (18,22). Tumor growth was inhibited by treatment with human HST-1/FGF-4 siRNA complexed with Atelocollagen. At 21 days following treatment, tumor volume in mice treated with siRNA complexed with Atelocollagen was smaller than that in the control mice treated with Atelocollagen alone (Figure 7A and B). In contrast, tumors treated with siRNA alone and control siRNA/Atelocollagen showed no significant volume reduction. Furthermore, the FGF-4 siRNA/Atelocollagen complex significantly inhibited the production of FGF-4 in the tumors (Figure 7C) and this inhibition lasted for 20 days. Therefore, the Atelocollagen-mediated siRNA transfer is a significant novel method for inhibition of tumor growth *in vivo*.

DISCUSSION

Silencing of gene expression by siRNAs is rapidly becoming a powerful tool for the genetic analysis of a wide variety of mammalian cells. Although in the original studies, the expression of siRNA in mammalian cells was achieved via the transfection of double-stranded oligonucleotides, subsequent studies described the limited duration of the gene silencing effect. To overcome this problem, the use of plasmids to achieve a long-term and stable expression of siRNA was established (23–25). In addition, several groups have described the use of adenoviral vectors (9), retroviral vectors (26) and self-inactivating lentiviral vectors (27) for siRNA delivery. However, viral vectors suffer from the problem of severe side effects. Although the 'hydrodynamic transfection method' and a liposome transfection method were recently reported for siRNA delivery into animals (8,28), none is suitable for clinical use. Therefore, the development of safe non-vector-based siRNA delivery systems is critical for the future of siRNA-based therapies. Here, we used an Atelocollagen-mediated siRNA transfer in an *in vitro* and *in vivo* germ cell tumor-suppression model. Because Atelocollagen allowed increased cellular uptake, nuclease resistance and prolonged release of siRNAs, Atelocollagen complexed with siRNA rather than siRNA alone or a polycation transfer method resulted in stronger gene silencing effects over other methods. It is known that Atelocollagen has the ability to transfer genes to both dividing and non-dividing

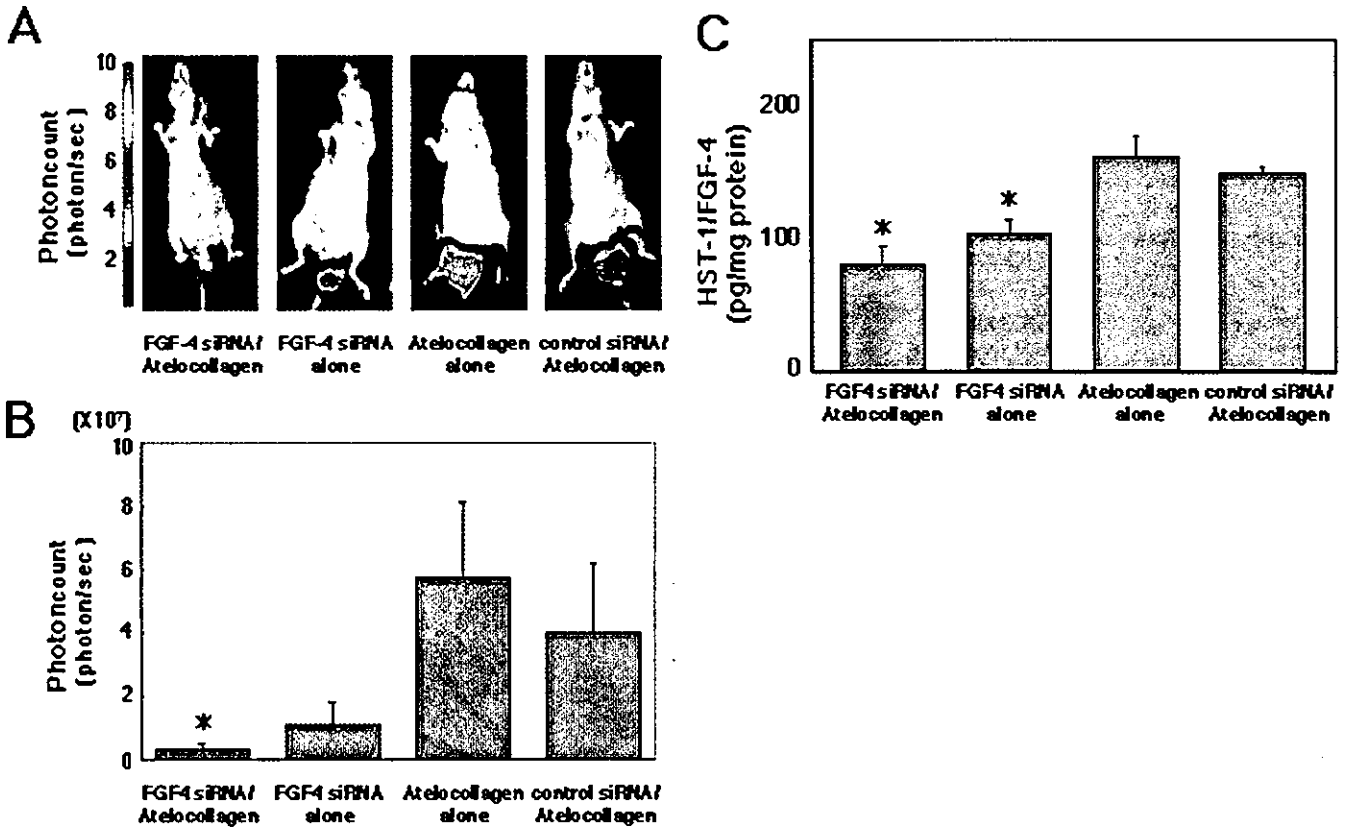

Figure 7. Effect of siRNA/Atelocollagen complex on the growth of a xenograft tumor. (A) Human HST-1/FGF-4 siRNA (2.5 μg) complexed with 0.5% Atelocollagen was transduced into an orthotopic germ cell tumor of NEC8 cells expressing the luciferase gene. Representative images at 21 days after treatment are shown. As a control, an Atelocollagen complex with non-specific control siRNA duplex that shows no silencing effect on human HST-1/FGF-4 was used (control siRNA/Atelocollagen). (B) Measurements of a xenograft tumor bioluminescence at 21 days after treatment. Data represent the mean ± SE. *, $P < 0.05$ versus Atelocollagen alone treatment. (C) Evaluation of HST-1/FGF-4 protein expression in tumor tissue extracts 3 days after treatment. Protein levels were quantified by ELISA. Data represent the mean ($n = 4$) ± SE. *, $P < 0.05$ versus Atelocollagen alone and control siRNA/Atelocollagen treatment.

cells. Thus, for clinical applications in RNAi therapy, an Atelocollagen-based siRNA transfer system represents an attractive method to achieve maximal function of siRNA-based gene silencing *in vivo*.

One technical problem associated with siRNA transfer *in vivo* is the targeting of siRNA delivery to a specific tissue. For this purpose, our Atelocollagen-based transfer method has great potential for site-specific transportation of target siRNAs because the complex of siRNA/Atelocollagen becomes solid when transplanted and remains so for a defined period *in vivo*. In addition, an Atelocollagen complex can be delivered as micro-particles for intravenous injection, making systemic delivery of siRNA possible. A recent report showed the potential for Atelocollagen-mediated systemic antisense therapeutics for inflammatory disease (29). Following *in vivo* administration, the incorporated siRNAs are slowly released over an extended period of time. This eliminates the need for multiple injections of siRNA and siRNA vectors, in lessened side effects.

Although siRNAs are thought to be too short to induce interferon expression, recent reports has shown that siRNA sequences and their method of delivery may trigger an interferon response (30,31). Therefore, alternative strategies are needed to reduce the induction of non-specific side effects. In this regard, our Atelocollagen-mediated non-vector transfer method is an attractive strategy to deliver siRNAs *in vivo*, since our Atelocollagen has low-toxicity and is low-immunogenic, and hence unlikely to stimulate interferon expression *in vivo*.

Finally, based on the ability of Atelocollagen to achieve the sustained release of siRNA and to enhance the stability of siRNA *in vivo*, our novel delivery method demonstrates potential for use as a therapeutic tool for the delivery of siRNA.

ACKNOWLEDGEMENTS

We thank Ms Kazumi Kimura, Ms Masako Hosoda and Ms Ayako Inoue for their excellent technical work. This work was supported in part by a Grant-in-Aid for the Second-Term Comprehensive 10-Year Strategy for Cancer Control, Health Science Research Grants for the Research on the Human Genome and Gene Therapy from the Ministry of Health, Labour and Welfare of Japan, a Grant-in-Aid for Scientific Research on Priority Areas Cancer from the Ministry of Education, Culture, Sports, Science and Technology, and the Program for Promotion of Fundamental Studies in Health Sciences of the Organization for Pharmaceutical Safety and Research of Japan.

REFERENCES

1. Fire,A., Xu,S., Montgomery,M.K., Kostas,S.A., Driver,S.E. and Mello,C.C. (1998) Potent and specific genetic interference by double-stranded RNA in *Caenorhabditis elegans*. *Nature*, **391**, 806–811.
2. Scherr,M., Morgan,M.A. and Eder,M. (2003) Gene silencing mediated by small interfering RNAs in mammalian cells. *Curr. Med. Chem.*, **10**, 245–256.
3. Elbashir,S.M., Harborth,J., Lendeckel,W., Yalcin,A., Weber,K. and Tuschl,T. (2001) Duplexes of 21-nucleotide RNAs mediate RNA interference in cultured mammalian cells. *Nature*, **411**, 494–498.
4. Lee,N.S., Dohjima,T., Bauer,G., Li,H., Li,M.J., Ehsani,A., Salvaterra,P. and Rossi,J. (2002) Expression of small interfering RNAs targeted against HIV-1 rev transcripts in human cells. *Nat. Biotechnol.*, **20**, 500–505.
5. Paul,C.P., Good,P.D., Winer,I. and Engelke,D.R. (2002) Effective expression of small interfering RNA in human cells. *Nat. Biotechnol.*, **20**, 505–508.
6. Simeoni,F., Morris,M.C., Heitz,F. and Divita,G. (2003) Insight into the mechanism of the peptide-based gene delivery system MPG: implications for delivery of siRNA into mammalian cells. *Nucleic Acids Res.*, **31**, 2717–2724.
7. Bertrand,J.R., Pottier,M., Vekris,A., Opolon,P., Maksimenko,A. and Malvy,C. (2002) Comparison of antisense oligonucleotides and siRNAs in cell culture and *in vivo*. *Biochem. Biophys. Res. Commun.*, **296**, 1000–1004.
8. Sorensen,D.R., Leirdal,M. and Sioud,M. (2003) Gene silencing by systemic delivery of synthetic siRNAs in adult mice. *J. Mol. Biol.*, **327**, 761–766.
9. Xia,H., Mao,Q., Paulson,H.L. and Davidson,B.L. (2002) siRNA-mediated gene silencing *in vitro* and *in vivo*. *Nat. Biotechnol.*, **20**, 1006–1010.
10. Tomar,R.S., Matta,H. and Chaudhary,P.M. (2003) Use of adeno-associated viral vector for delivery of small interfering RNA. *Oncogene*, **22**, 5712–5715.
11. Matta,H., Hozayev,B., Tomar,R., Chugh,P. and Chaudhary,P.M. (2003) Use of lentiviral vectors for delivery of small interfering RNA. *Cancer Biol. Ther.*, **2**, 206–210.
12. Stenzel,K.H., Miyata,T. and Rubin,A.L. (1974) Collagen as a biomaterial. *Annu. Rev. Biophys. Bioeng.*, **3**, 231–253.
13. Ochiya,T., Nagahara,S., Sano,A., Itoh,H. and Terada,M. (2001) Biomaterials for gene delivery: atelocollagen-mediated controlled release of molecular medicines. *Curr. Gene Ther.*, **1**, 31–52.
14. Honma,K., Ochiya,T., Nagahara,S., Sano,A., Yamamoto,H., Hirai,K., Aso,Y. and Terada,M. (2001) Atelocollagen-based gene transfer in cells allows high-throughput screening of gene functions. *Biochem. Biophys. Res. Commun.*, **289**, 1075–1081.
15. Ochiya,T., Takahama,Y., Nagahara,S., Sumita,Y., Hisada,A., Itoh,H., Nagai,Y. and Terada,M. (1999) New delivery system for plasmid DNA *in vivo* using atelocollagen as a carrier material: the Minipellet. *Nature Med.*, **5**, 707–710.
16. Sano,A., Maeda,M., Nagahara,S., Ochiya,T., Honma,K., Itoh,H., Miyata,T. and Fujioka,K. (2003) Atelocollagen for protein and gene delivery. *Adv. Drug Deliv. Rev.*, **55**, 1651–1677.
17. Yoshida,T., Tsutsumi,M., Sakamoto,H., Miyagawa,K., Teshima,S., Sugimura,T. and Terada,M. (1988) Expression of the HST1 oncogene in human germ cell tumors. *Biochem. Biophys. Res. Commun.*, **155**, 1324–1329.
18. Vooijs,M., Jonkers,J., Lyons,S. and Berns,A. (2002) Noninvasive imaging of spontaneous retinoblastoma pathway-dependent tumors in mice. *Cancer Res.*, **62**, 1862–1867.
19. Hirai,K., Sasaki,H., Sakamoto,H., Takeshita,F., Asano,K., Kubota,Y., Ochiya,T. and Terada,M. (2003) Antisense oligodeoxynucleotide against HST-1/FGF-4 suppresses tumorigenicity of an orthotopic model for human germ cell tumor in nude mice. *J. Gene Med.*, **5**, 951–957.
20. Konishi,H., Ochiya,T., Sakamoto,H., Tsukamoto,M., Saito,I., Muto,T., Sugimura,T. and Terada,M. (1995) Effective prevention of thrombocytopenia in mice using adenovirus-mediated transfer of HST-1 (FGF-4) gene. *J. Clin. Invest.*, **96**, 1125–1130.
21. Takei,Y., Kadomatsu,K., Yuzawa,Y., Matsuo,S. and Muramatsu,T. (2004) A small interfering RNA targeting vascular endothelial growth factor as cancer therapeutics. *Cancer Res.*, **64**, 3365–3370.
22. Rehemtulla,A., Stegman,L.D., Cardozo,S.J., Gupta,S., Hall,D.E., Contag,C.H. and Ross,B.D. (2000) Rapid and quantitative assessment of cancer treatment response using *in vivo* bioluminescence imaging. *Neoplasia*, **2**, 491–495.
23. Miyagishi,M. and Taira,K. (2002) U6 promoter-driven siRNAs with four uridine 3′ overhangs efficiently suppress targeted gene expression in mammalian cells. *Nat. Biotechnol.*, **20**, 497–500.
24. Hasuwa,H., Kaseda,K., Einarsdottir,T. and Okabe,M. (2002) Small interfering RNA and gene silencing in transgenic mice and rats. *FEBS Lett.*, **532**, 227–230.
25. Pekarik,V., Bourikas,D., Miglino,N., Joset,P., Preiswerk,S. and Stoeckli,E.T. (2003) Screening for gene function in chicken embryo using RNAi and electroporation. *Nat. Biotechnol.*, **21**, 93–96.
26. Hemann,M.T., Fridman,J.S., Zilfou,J.T., Hernando,E., Paddison,P.J., Cordon-Cardo,C., Hannon,G.J. and Lowe,S.W. (2003) An epi-allelic series of p53 hypomorphs created by stable RNAi produces distinct tumor phenotypes *in vivo*. *Nature Genet.*, **33**, 396–400.
27. Rubinson,D.A., Dillon,C.P., Kwiatkowski,A.V., Sievers,C., Yang,L., Kopinja,J., Rooney,D.L., Ihrig,M.M., McManus,M.T., Gertler,F.B. *et al.* (2003) A lentivirus-based system to functionally silence genes in primary mammalian cells, stem cells and transgenic mice by RNA interference. *Nature Genet.*, **33**, 401–406.
28. Song,E., Lee,S.K., Wang,J., Ince,N., Ouyang,N., Min,J., Chen,J., Shankar,P. and Lieberman,J. (2003) RNA interference targeting Fas protects mice from fulminant hepatitis. *Nature Med.*, **9**, 347–351.
29. Hanai,K., Kurokawa,T., Minakuchi,Y., Maeda,M., Nagahara,S., Ito,H., Ochiya,T. and Sano,A. (2004) Potential for atelocollagen-mediated systemic antisense therapeutics for inflammatory disease. *Human Gene Ther.*, **15**, 263–272.
30. Bridge,A.J., Pebernard,S., Ducraux,A., Nicoulaz,A.L. and Iggo,R. (2003) Induction of an interferon response by RNAi vectors in mammalian cells. *Nature Genet.*, **34**, 263–264.
31. Sledz,C.A., Holko,M., de Veer,M.J., Silverman,R.H. and Williams,B.R. (2003) Activation of the interferon system by short-interfering RNAs. *Nature Cell Biol.*, **5**, 834–839.

アテロコラーゲンを用いた合成 small interfering RNA の *in vivo* 導入技術

竹下文隆，水口佳子，落谷孝広

はじめに

近年のゲノムプロジェクトの完了によってヒトの全遺伝子配列が解読され，また数多くの疾患関連遺伝子が同定され続けている現在，特定の遺伝子を標的とした治療法，創薬の開発が盛んに行われている．なかでも注目されているのは，特異的転写後抑制効果を発揮するsmall interfering RNA（siRNA）の遺伝子治療への応用である．しかしsiRNAは*in vitro*においては非常にすぐれた特異的転写後抑制効果を示すが，*in vivo*においては血清中のヌクレアーゼにより速やかに分解されてしまうため，その持続期間が限られており，*in vivo*での効果的なデリバリーシステムの開発が求められている．無論，遺伝子治療を見据えるためには，副作用を最小限にとどめなければならない．これまでに報告されているsiRNAの生体へのデリバリー方法とそれらの問題点を表にまとめた．われわれは，生体親和性材料であるアテロコラーゲンをsiRNAのキャリアーとして用いた，*in vivo*デリバリーシステムの開発を行っている．アテロコラーゲンによる遺伝子導入は，*in vitro*においても有効な手段であるが[1]，われわれはこれまでに，プラスミドやアデノウイルスベクターとアテロコラーゲンとの複合体を実験動物に投与し，DNA発現を誘導することに成功した[2)3)]．またアンチセンスオリゴヌクレオチドとアテロコラーゲンとの複合体については，移植した腫瘍への直接投与による腫瘍の増殖，転移の抑制効果や[4]，尾静脈投与により末梢部位で実験的に惹起した炎症が抑制されることを報告してきた[5]．アテロコラーゲンは，核酸と混合し複合体を形成させると，生体中の分解酵素から核

表　報告されているsiRNAの生体へのデリバリーシステムと問題点

ベクター	種類	問題点
非ウイルスベクター（プラスミドベクター）	カチオン性リポソーム	・毒性が懸念される
	急速静注法	ヒトへの適用は困難
ウイルスベクター	アデノウイルスベクター	・毒性が懸念される
	レトロウイルスベクター	・生体の免疫応答を惹起する可能性あり

Atelocollagen-mediated effective *in vivo* transfer method for synthetic small interfering RNAs
Fumitaka Takeshita[1] /Yoshiko Minakuchi[2] /Takahiro Ochiya[1] : Section for Studies on Metastasis, National Cancer Center Research Institute[1] /Formulation Research Laboratories, Sumitomo Pharmaceutical Co. Ltd.[2]（国立がんセンター研究所がん転移研究室[1] /住友製薬製剤技術研究所[2]）E-mail : futakesh@gan2.res.ncc.go.jp

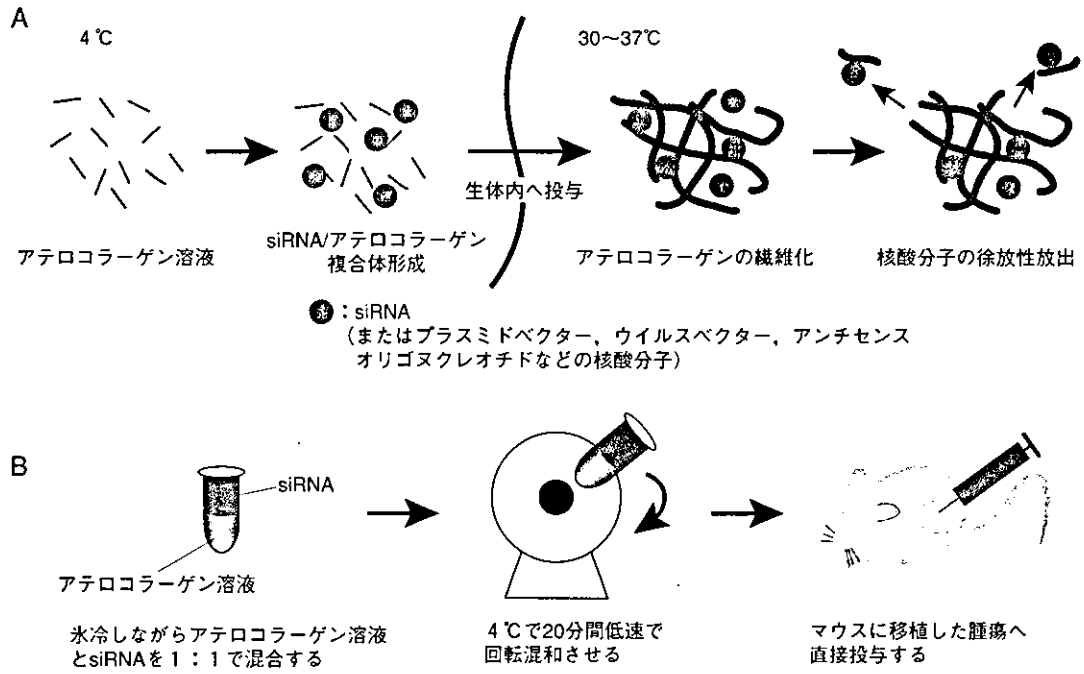

図1　siRNA/アテロコラーゲン複合体
A）siRNA/アテロコラーゲン複合体の形成と生体内での徐放性放出の模式図．B）siRNA/アテロコラーゲン複合体の調製から投与までの流れ

酸を保護する作用があり[3) 6)]，siRNAのキャリアーとしても非常に適していると考えられる．またわれわれは，siRNAデリバリーシステムの開発に，*in vivo* イメージングシステムを活用している[7)]．このシステムは，ルシフェラーゼを安定に発現する細胞を動物に移植し，ルシフェラーゼの発光を検出することにより，移植した細胞の増殖，浸潤，転移等の挙動を，動物を生かしたまま，経時，経日的に観察できる方法であり，今後，さまざまな創薬開発に有用であると期待される．本稿では，ルシフェラーゼ発現マウスメラノーマ細胞を，ヌードマウスの皮下に移植し，生着後のメラノーマに直接，ルシフェラーゼに対するsiRNAとアテロコラーゲンの複合体を投与した実験系を紹介させていただく．

原理

❶ アテロコラーゲンとは

アテロコラーゲンは，仔ウシの真皮のⅠ型コラーゲンより精製されるが，コラーゲン分子の両端に存在する，主要抗原部位であるテロペプチドというアミノ酸配列を，ペプシン処理により除去して製したバイオマテリアルで，抗原性はきわめて低く，医療材料としても使用されている[3)]．

❷ アテロコラーゲンの性状と核酸との複合体の形成

アテロコラーゲンは，分子量約300 kD，長さ約300 nm，直径約1.5 nmの棒状の構造を示す．アテロコラーゲンは，4℃以下の低温では液体（ゲル状）であるので，核酸溶液と混合することが可能で，核酸分子と静電気的に結合し，粒子状の複合体を形成する．この核酸とアテロコラーゲンとの複合体の粒子径については，両者の混合比を変化させることにより調節が可能である．アテロコラーゲンの濃度が高いと繊維化傾向が強く，生体に投与した際に局在性にすぐれ，また低濃度では数百nmと粒子径が小さいことから，細胞へ取り込まれやすいと考えられる[6)]．細胞中に取り込まれた複合体は，生体由来の酵素などによる核酸の分解を防御するが，アテロコラーゲンそのものは徐々

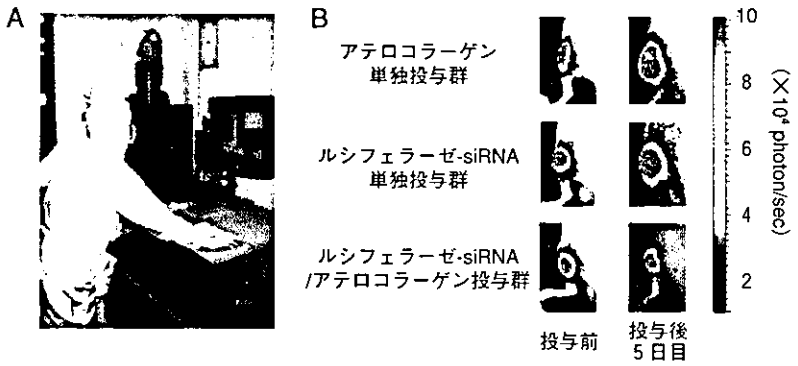

図2 *in vivo*イメージングシステムを用いた，ルシフェラーゼ発光抑制実験
A）*in vivo*イメージングシステムによる実験風景．B）ルシフェラーゼ-siRNA/アテロコラーゲン複合体投与によるルシフェラーゼ発光抑制効果：ルシフェラーゼを安定に発現するメラノーマ細胞を，ヌードマウスの皮下に移植し，ルシフェラーゼ-siRNA/アテロコラーゲン複合体投与によるルシフェラーゼの発光抑制効果を*in vivo*イメージングにより測定した

に分解され核酸分子を放出するため，徐放性に，そして結果的に持続性に優れた作用を示す（図1 A）．

❸ *in vivo*イメージングシステム

われわれが用いた*in vivo*イメージングシステムは，動物体内においてルシフェラーゼと基質であるルシフェリンとの反応によって産生される発光を，冷却装置付き超高感度CCDカメラにより検出し，コンピュータによって可視化する装置である[7]．さらに発光量の数値化が可能で，ルシフェラーゼを発現する細胞を動物に移植して測定を行えば，細胞の増減を定量することも可能となる．測定は動物をガス麻酔下で行うため同一の動物を経時，経日的に行える（図2 A）．

準備

- ルシフェラーゼ発現マウスメラノーマ細胞（B16-F10-Luc-G5, Xenogen Corp.）：pGL3 controlベクター（Promega）を導入した，安定にルシフェラーゼを発現する細胞．
- ヌードマウス
- PBS（Ca，Mg不含，DEPC処理済も必要）
- 3.5％アテロコラーゲン（株式会社高研）
- Luciferase GL3 Duplex（Dharmacon）：ルシフェラーゼの発現を特異的に抑制することが確認されている合成siRNA[8]．脱保護，脱塩精製グレード．
- *in vivo*バイオイメージング装置（IVIS™ Imaging System，住商バイオサイエンス株式会社，Xenogen Corp.）
- ルシフェリン（D-Luciferin, Firefly, potassium salt, Xenogen Corp）：15 mg/mlでPBSに溶解し，0.2 μmシリンジフィルターを通して滅菌する．

プロトコール

1 1日目

【細胞の移植】

ルシフェラーゼ発現マウスメラノーマ細胞をトリプシン処理で回収し，PBSに懸濁，ヌードマウスの皮下に部位あたり5×10^5 cells/0.05 m*l*で移植する．

2 2日目

【アテロコラーゲンの希釈】(siRNAの投与前日に行う)

3.5%アテロコラーゲンを秤量し[※1]，最終濃度1%になるようにPBSで希釈する．4℃で泡立たない速度で一晩回転混和させる．

3 3日目

【*in vivo*イメージング】(腫瘍の生着の確認と投与前のデータの取得)

メラノーマを移植したマウスにルシフェリンを体重1 gあたり0.01 m*l*腹腔内投与し，10～15分後にイメージングを行う．

【siRNA/アテロコラーゲンの調製】

1%アテロコラーゲンに等量の10 μM Luciferase GL3 Duplexを添加し，4℃で20分間，低速で回転混和させる（図1 B)．

【siRNA/アテロコラーゲンの投与】

siRNA/アテロコラーゲン混合液を，ヌードマウスの腫瘍を移植した部位に，0.2 m*l*投与する[※2]．

4 4日目以降

【*in vivo*イメージング】

siRNAの投与から経日的にイメージングを行い，発光量の減弱から，siRNAの効果を検討する．

※1　3.5%アテロコラーゲンは粘性が高くピペットで正確に量り取れないので重量で秤量する．比重は1として計算してよい．

※2　直径約3 mmの大きさの腫瘍あたり13.3 μg投与したことになる．

実験例

イメージングの結果の代表例を図2 Bに示した．アテロコラーゲン単独投与群では，投与前と投与後5日目では，メラノーマの増殖と共に発光量も増加している．ルシフェラーゼ-siRNAの単独投与でルシフェラーゼの発光の抑制はほとんど確認されなかったが，siRNAとアテロコラーゲン複合体の投与では抑制効果が観察された．

おわりに

今回用いたLuciferase GL3 Duplexは，ルシフェラーゼの発現に対して抑制効果を示すが，メラノーマの増殖には影響しないとされている．よって，今回の実験は腫瘍抑制が目的ではなく，投与した合成siRNAが生体内で機能するかの検討が目的である．メラノーマまたは他の腫瘍においても，ルシフェラーゼ遺伝子を導入し，その腫瘍の増殖，転移などに関与する遺伝子に特異性をもつsiRNAを設計し，今回のような実験系で試験すれば，抑制効果をリアルタイムで検討することが可能であり，創薬の開発などに有力な手段となりうると考えられる．また，名古屋大学の武井博士らもアテロコラーゲンに着目し，siRNA/アテロコラーゲン複合体による，マウスに皮下移植した腫瘍の抑制効果を示している．

現在は，癌以外にも血管系や神経系の疾患，感染症，自己免疫疾患，肥満や糖尿病などの治療へsiRNAを応用する研究がなされ[9]，これまでのDNA発現の知識を生かし，組織または細胞特異的発現プラスミドベクターや，ウイルスベクターの開発が盛んに行われている．われわれは，アテロコラーゲンとアデノウイルスベクターの複合体が，免疫応答性を抑え，複数回投与を可能にすることを確認しており[3]，siRNA発現ウイルスベクターについても，アテロコラーゲンとの複合体を形成させることで，副作用を抑える可能性が高いと予想される．また現在われわれは，アンチセンスオリゴの全身投与にもアテロコラーゲンの適用が可能であった結果をふまえ[5]，アテロコラーゲンに修飾を施し，腫瘍細胞に対する特異性を高めた，転移性腫瘍を標的としたデリバリーシステムの開発を検討中である．

文献

1）Honma, K. et al.：Biochem. Biophys. Res. Commun., 289：1075-1081, 2001
2）Ochiya, T. et al.：Nature Med., 5：707-710, 1999
3）Ochiya, T. et al.：Curr. Gene Ther., 1：31-52, 2001
4）Hirai, K. et al.：J. Gene Med., 5：951-957, 2003
5）Hanai, K. et al.：Human Gene Ther., in press (2004)
6）Sano, A. et al.：Adv. Drug Deliv. Rev., 55：1651-1677, 2003
7）落谷孝広，他：Bioベンチャー Vol. 3 No. 6：71-88, 2003
8）Elbashir, S. M. et al.：Nature, 411：494-498, 2001
9）Milhavet, O. et al.：Pharmacol. Rev., 55：629-648, 2003

High Performance Gene Delivery Polymeric Vector: Nano-Structured Cationic Star Polymers (Star Vectors)

Yasuhide Nakayama[1,*], Takeshi Masuda[1], Makoto Nagaishi[1], Michiko Hayashi[1], Moto Ohira[2] and Mariko Harada-Shiba[2]

[1]*Department of Bioengineering, National Cardiovascular Center Research Institute,* [2]*Department of Bioscience, National Cardiovascular Center Research Institute, 5-7-1 Fujishiro-dai, Suita, Osaka 565-8565, Japan*

Abstract: Nano-structured hyperbranched cationic star polymers, called star vectors, were molecularly designed for a novel gene delivery non-viral vector. The linear and 3, 4 or 6 branched water-soluble cationic polymers, which had same molecular weight of ca. 18,000, were synthesized by iniferter (initiator-transfer agent-terminator)-based photo-living-radical polymerization of 3-(*N,N*-dimethylamino)propyl acrylamide, initiated from respective multi-dithiocarbamate-derivatized benzenes as an iniferter. All polymers produced polyion complexes 'polyplexes' by mixing with pDNA (pGL3-control plasmid), in which the particle size was ca. 250 nm in diameter [the charge ratio < 2/1 (vevtor/pDNA)] and ca. 150 nm (the charge ratio > 2.5/1), and the ζ-potential was ca. +10 mV (the charge ratio > 1/1). When COS-1 cells were incubated with the polyplexes 12h after preparation under the charge ratio of 5/1, higher gene expression was obtained as an increase in branching, with a little cytotoxicity. The relative gene expression to the linear polymer was about 2, 5, and 10 times in 3-, 4-, and 6-branched polymers, respectively. The precise change in branching of polymers enabled the control of the gene transfer activity.

Keywords: Non-viral vector, star polymer, polyplex, branched polymer, gene transfection, molecular design.

INTRODUCTION

The cationic polymers, which can generate nano-particles by formation of polyion complexes 'polyplexes' with DNA irrespective of its size and kind, are highly expected as one of the major materials for non-viral vectors [1-4]. However, the primary obstacle toward implementing an effective gene therapy using the cationic polymers remains their relatively inefficient gene transfection *in vivo* than virus vectors.

To achieve an enhancement of gene transfection using cationic polymers, numerous studies have been performed by various approaches; e.g., the chemical synthetic engineering approach in which the kind and composition of the polymers are modified [5,6], biochemical approach in which targeting ligands such as galactose, mannose, transferring, or antibodies into the polymers [7-11], functional molecular engineering approach in which stimulus-response polymers with light and thermal reactivity are designed as high performance vectors [12-14], and physical engineering approach in which physical stimulation with electroporation, gene gun, ultrasound and hydrodynamic pressure are provided at the transfection [2,15,16]. However, few studies in the molecular structure of cationic polymers, which are usually synthesized by conventional radical polymerization, has been reported, except for the effects of changes in the polymer chain length and composition of polymers [17-20] and complex multi-branching polymers, of which structural analysis is impossible [21-24]. Since precise molecular design, including the molecular weight and three-dimensional structure, by conventional radical polymerization was quite difficult in general, the systematic structure-dependency of cationic polymers in gene transfection has not been established.

In this study, for examination of the effects of the molecular structure on gene expression we designed novel cationic polymers with star-shaped and symmetric structure, which is determined by 2-parameters, the degree of branching and chain length. Molecular design was performed by the iniferter (acts as *ini*tiator-trans*fer* agent-*ter*minator)-based photo-living-radical polymerization method pioneered by Otsu *et al.* [25-30]. An iniferter, benzyl *N,N*-diethyldithiocarbamate (DC) is dissociated into a benzyl radical and a dithiocarbamyl radical by ultraviolet light (UV) irradiation. The reaction involving an *N,N*-diethyldithiocarbamyl radical favors chain termination with a growing polymer chain radical end rather than a reaction with a vinyl monomer, whereas a benzyl radical reacts with a vinyl monomer to produce a polymer. These reactions proceed only during irradiation. Therefore, the chain length of the growing polymer is controlled by irradiation condition such as irradiation time or light intensity and the composition of the solution. We previously used the living radical polymerization for designing of various surface graft architectures [31-34] controlling the chain length, block graft chain, gradient chain length and regionally graft polymerized pattern surface. As the first step of the study, star polymers of the same molecular weight at a precise degree of branching of 0, 3, 4, and 6 were synthesized. The effects of the degree of branching on gene expression by measuring the luciferase activity were examined.

*Address correspondence to this author at the Department of Bioengineering, National Cardiovascular Center Research Institute, 5-7-1 Fujishiro-dai, Suita, Osaka 565-8565, Japan; Tel: +81-6-6833-5012; Fax: +81-6-6872-8090; E-mail: nakayama@ri.ncvc.go.jp

1567-2018/05 $50.00+.00

MATERIALS AND METHODS

Materials

Benzyl chloride, 2,4,6-tris(bromomethyl)mesitylene, 1,2,4,5-tetrakis(bromomethyl)benzene, and hexakis(bromomethyl)benzene were obtained from Sigma-Aldrich (Milwaukee, WI). Sodium *N,N*-diethyldithiocarbamate and *N,N*-dimethyaminopropyl acrylamide were purchased from Wako Pure Chemical Ind. Ltd. (Osaka, Japan). Solvents and other reagents, all of which were of special reagent grade, were obtained from Wako and used after conventional purification. Plasmid DNA (pGL3-control), which contains the firefly luciferase gene, was obtained from Promega Inc., (Tokyo, Japan). ExGen 500 [poly(ethylene imine)] was obtained from Euromedex Inc., (Cedex, France).

Synthesis of Cationic Star Polymers

Cationic polymers including linear and three types of star polymers with 3, 4, or 6 branches per molecule were prepared by iniferter-based photo-living-radical polymerization of 3-(*N,N*-dimethylamino)propyl acrylamide as a monomer from respective inifeters such as benzyl *N,N*-diethyldithiocarbamate, 2,4,6-tris (*N,N*-diethyldithiocarbamylmethyl)mesitylene, 1,2,4,5- tetrakis(*N,N*-diethyldithiocarbamylmethyl)benzene, and hexakis (*N,N*-diethyldithiocarbamylmethyl)benzene, which were obtained by *N,N*-diethyldithiocarbamylation from respective benzyl halogenate derivatives such as benzyl chloride, 2,4,6-tris (bromomethyl)mesitylene, 1,2,4,5-tetrakis(bromomethyl) benzene, and hexakis(bromomethyl)benzene.

The general preparation method of iniferter is followed. An ethanol solution (10 ml) of chloromethyl benzene (4.8 g, 38 mmol) was added to an ethanol solution (50 ml) of sodium *N,N*-diethyldithiocarbámate (10.3 g, 46 mmol) at 0°C. After the mixture was stirred at room temperature for 24 h, the resulting sodium chloride was separated by filtration. The filtrate was concentrated under reduced pressure. The residue was added into 150 ml of water and extracted with ether (200 ml x 2) and washed successively with deionized water (100 ml x 3), followed the separation of the organic layer, drying over $MgSO_4$, condensation to give benzyl *N,N*-diethyldithiocarbamate: yield, 17.6g (93%); ^{1}H NMR (DMSO-d_6 with Me_4Si) δ 7.34 (m, 5H, C_6H_5), 4.54 (s, 2H, CH_2-S), 4.05 (q, 2H, N-CH_2), 3.73 (q, 2H, N-CH_2), 1.28 (m, 6H, CH_2CH_3).

The general procedure of iniferter-induced photo-living-radical polymerization is followed. A methanol solution (20 ml) of benzyl *N,N*-diethyldithiocarbamate (24 mg, 0.1 mmol) and 3-(*N,N*-dimethylamino)propyl acrylamide (3.9 g, 25 mmol) was placed into 50 ml quartz crystal tube. A stream of dry nitrogen was introduced through a gas inlet to sweep the tube for 5 min or more. The solution was then irradiated for 30 min with a 200 W Hg lamp (SPOT CURE, USHIO, Tokyo, Japan) in nitrogen atmosphere at 20~25 °C. Light intensity was set to 1 mW/cm^2 at the wavelength of 250 nm (UVR-1, TOPCON, Tokyo, Japan). The reaction mixture was concentrated under reduced pressure. The residue was dissolved in a small amount of methanol. The precipitate, obtained by the addition of a large amount of ether, was separated by filtration. Reprecipitation was performed in the methanol-ether system. The last precipitate was dried in a vacuum to yield poly[3-(*N, N*-dimethylamino)propyl acrylamide] as a white powder. The molecular weight, determined by GPC analysis, was 18,000 g mol^{-1}. ^{1}H NMR (DMSO-d_6 with Me_4Si) δ 7.60 (br, 1H, N-*H*), 3.22 (br, 2H, NH-CH_2), 2.30 ((br, 2H, $N(CH_3)_2$-CH_2), 2.15 (br, 6H, N-CH_3), 1.65 (br, 2H, CH_2-CH_2).

General Methods

GPC analysis was carried out on a RI-8012 (TSK_{gel} α-3000 and α-5000; Tosoh, Tokyo, Japan) after calibration with standard polyethylene glycol samples. The eluent was *N,N*-dimethylformamide. ^{1}H-NMR spectra were obtained on a Valian Gemini-300 (300 MHz) spectrometer (Tokyo, Japan). All ^{1}H-NMR spectra were recorded in DMSO-d_6 solutions using tetramethylsilane as the internal standard. Dynamic light scattering (DLS) measurements were carried out using a DLS-8000 instrument (Otsuka Electrinics, Tokyo, Japan). An Ar ion laser (λ_0 = 488 nm) was used as the incident beam. The sample was prepared by direct mixing of pDNA solution and the polymer in Tris-HCl buffer (pH 7.4). The DNA concentration of the mixture was then adjusted to 23 μg cm^{-3}.

Cell Culture and Transfection

COS-1 cells (ca. 3 x 10^4 cells per well) were seeded prior to treatment in 24-well plates and grown for 24 h in DMEM (Gibco, Invitrogen Corp., Carlsbad, CA) containing 10% fetal calf serum (Hyclone Laboratories Inc., Logan, UT), penicillin (200 units/ml, ICN Biomedicals Inc., Aurora, OH), and streptomycin (200 mg/ml, ICN) in an atmosphere of 5% CO_2 at 37 °C. Transfections were performed with 0.5 μg of plasmid DNA (pGL3-control) in 24-multi well dishes in 0.2 ml of OPTI-MEM I (Gibco). After 3 h of incubation, the cells were washed once with PBS, and cultured in 1 ml of DMEM containing 10% fetal calf serum for an additional 48 h. The medium was removed and the cells were washed twice with PBS. The cells were lysed with 0.2 ml of cell lysis buffer (Promega, Madison, WI) and mixed by vortexing. The lysate was centrifuged at 15,000 rpm for 1 min at 4 °C and 5 μl of the supernatant was analyzed for luciferase activity using a Luminous CT-9000D (Dia-Iatron, Tokyo, Japan) luminometer. The relative light unit/s (RLU) were converted into the amount of luciferase (pg) using a luciferase standard curve, which was obtained by diluting recombinant luciferase (Promega) in lysis buffer. The protein concentrations of cells lysates were measured by Bio-Rad protein assay (BIO-RAD, Hercules, CA) using bovine serum albumin as a standard. The expressed luciferase represented the amount (mole quantity), which is standardized for total protein content of cell lysate. The data are presented as means±S.D. (n=5).

Cytotoxicity

Cytotoxicity was assessed by cell viability assay using WST-8 method (Dojindo, Kumamoto, Japan). COS-1 cells were seeded 24 h prior to treatment in 96-well plates at 5,000 cells per well. Cells were treated with the same conditions used for luciferase assays, with a volume of 6.2 μl of the transfection mixture including 0.124 μg of pDNA added to

each well. Cells were treated with the appropriate conditions for 3 h, washed once with PBS, and cultures in 50 μl of DMEM (Gibco) containing 10% fetal calf serum for an additional 24 h. Each well was added with 10 μl of WST-8 reagent (5 mmol/l). After 2 h of incubation at 37 °C, absorbance at 450 nm was read in a BIO-RAD microplate reader (Model 680). The data are presented as means±S.D. (n=5).

RESULTS AND DISCUSSION

Preparation of Cationic Star Polymers

Four kinds of cationic polymers, consisting of one linear polymer and three star polymers precisely controlled the degree of branching to 3, 4, and 6, were molecularly designed (Fig. 1). The polymers were synthesized by the iniferter living radical polymerization using respective initiators, multi-dithiocarbamate-derivatized benzenes, which were prepared corresponding to the degree of branching. As the monomer, a cationic vinyl monomer with tertiary amino residues, 3-(*N,N*-dimethylamino)propyl acrylamide was used. Since polymerization could proceed only during irradiation, the chain length of the polymers could be easily controlled by the irradiation condition and the composition of the solution. One linear and three kinds of star polymers with a molecular weight of about 18,000 with low polydispersity of about 1.5, irrespective of the degree of branching, were obtained. Therefore, the chain length in the polymers was set to about 6,000 with a degree of branching of 3, about 4,500 with a degree of branching of 4, and about 3,000 with a degree of branching of 6.

Polyplex Formation

When aqueous solutions of all obtained branched cationic polymers with same molecular weight were mixed with a Tris-HCl buffered saline of pDNA, marked high scattering intensity in quasi-elastic (dynamic) light scattering (DLS) measurements was immediately observed regardless of the degree of branching, indicating polyplexes formation from all cationic polymers. It was considered that the polyplexes formed by electrostatic interactions are same as other cationic polymeric vectors. The particle sizes of the polyplexes were measured using DLS. The DLS measurements showed that the cumulant diameter of the polyplexes was about 250 nm at a charge ratio less than 2/1 (vector/pDNA) and decreased to about 150 nm at a charge ratio more than 2.5/1(vector/pDNA). However, the particle

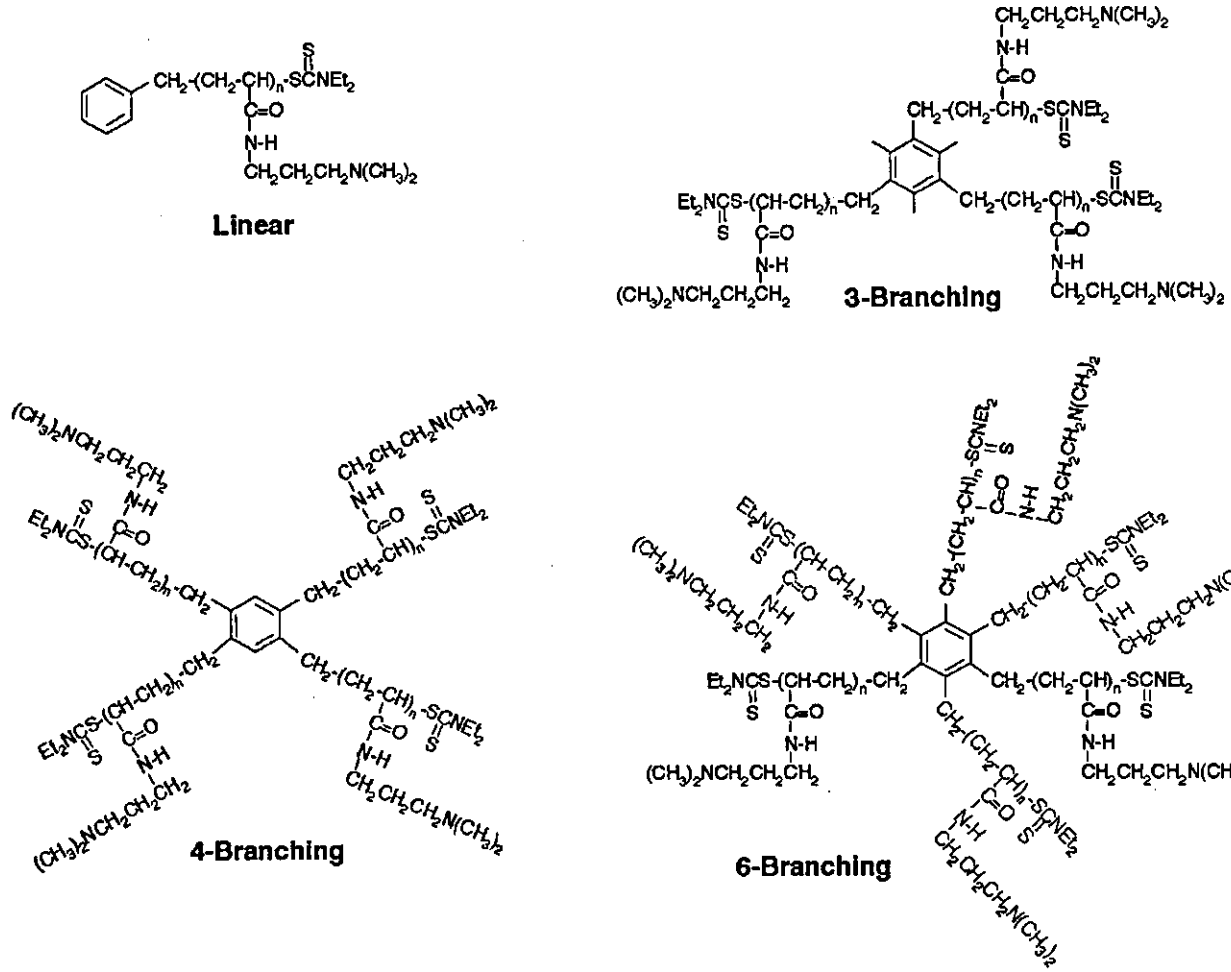

Fig. (1). Structural formulas of the star polymers, which were synthesized by iniferter-induced photo living radical polymerization of 3-(*N,N*-dimethylamino)propyl acrylamide from the respective multi-iniferters, *N,N*-diethyldithiocarbamate-derivatized benzenes.

sizes of the polyplexes were not significantly affected by the branching. In addition, ζ-potentials of pDNA polyplexes with the cationic polymers were measured to examine their electric property. The ζ-potential of the pDNA polyplexes was about +10 mV at a charge ratio more than 1/1(vector/pDNA). The difference in ζ-potential value between the polymers was little in each branching. Therefore, it can be said that there is little difference in physiochemical properties of the polyplexes produced from cationic polymers with different branching.

Cytotoxicity

Cytotoxicity of the pDNA polyplexes with the 6-branching polymer to COS-1 cells was studied by the cell survival rate using the WST-8 method. As shown in (Fig. 2) the cytotoxicity of the polyplexes was negligible up to a charge ratio of 5/1 (vector/pDNA). At charge ratios more than 5/1, the cytotoxicity was gradually reduced, and it was about 60% at a charge ratio of 20/1 (vector/pDNA).

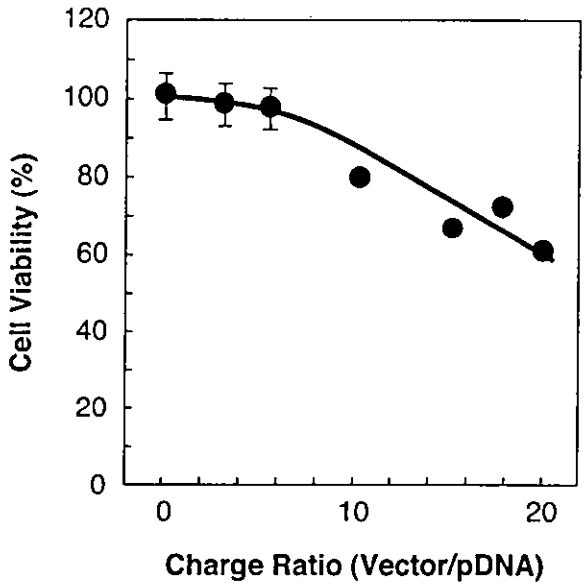

Fig. (2). Cytotoxicity of the polyplexes obtained immediately after mixing of DNA (pGL3-control) and 6-branching star polymer under the changing of a charge ratio (vector/pDNA), which was determined by cell viability assay of COS-1 cells using a WST-8 method. The data are presented as means±S.D. (n=5).

Gene Expression and Cell Viability

Gene transfer activity of the cationic polymers with same molecular weight of about 18,000 was examined and compared with that of ExGen 500 [35,36], which was one of major commercially available typical cationic polymeric vectors as a positive control. Figure 3 shows gene transfer activity of the cationic polymers at the charge ratio of 5/1 (vector/pDNA) in COS-1 cells. When pDNA alone was transfected, little luciferase activity was observed (data not shown). On the other hand, the luciferase was produced in all pDNA polyplexes. The enhancement of gene transfer activity in the use of the polyplexes may be due to acceleration of cellular uptake of pDNA polyplexes by

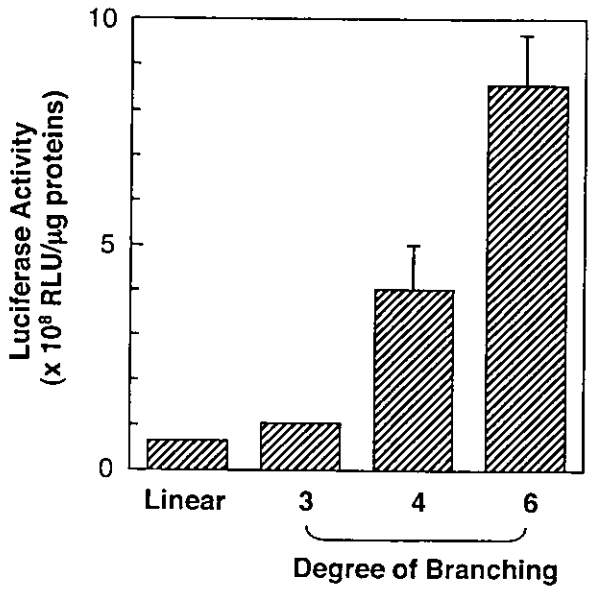

Fig. (3). Effect of branching of the star polymers on the level of luciferase gene transfer activity in COS-1 cells. COS-1 cells were treated with the polyplexes prepared by mixing of the star polymers and DNA (pGL3-control) under a charge ratio of 5/1 (vector/pDNA) 12 h after those preparation. The expression level was increased with increases in the degree of branching. The data are presented as means±S.D. (n=5).

endocytosis and endosomal release of the polyplexes by the proton sponge effect [37,38] in endosomes, similar to the other cationic polymers. The gene transfer activity of the pDNA polyplexes with the non-branched, linear cationic polymer was lowest, which was comparable with that of ExGen 500. However, the activity was increased by stage, corresponding to the degree of branching. The relative transfer activity to the linear polymer was about 2, 5 and 10 times in 3-, 4- and 6-branched polymers, respectively. As an increase in the degree of branching the transfer activity was almost exponentially increased. It can be said that the highly branched polymer called star vectors is useful for a gene delivery vector.

Cationic polymer-mediated transfection should overcome three major barriers for transfection, which includes binding of pDNA polyplexes to cell surface, endosormal release, and entry of pDNA into the nucleus. These barriers are strongly depended on the physicochemical properties of polyplexes such as net charge and particle size. Therefore, such properties markedly determine transfection efficiency. However, in the present study, transfection efficiency was strongly affected with the branching degree regardless of almost same physcochemical properties in pDNA polyplexes formed from the all branched polymers. The branching degree-dependent transfer activity changing may be estimated below. As an increase in the degree of branching the density of cationic charges in the branched polymers is increased. Higher charge density may affect the formation of higher compaction of pDNA polyplexes. The condensed pDNA polyplexes thus obtained may be stable in endosomes and also in aqueous media, which may prevent degradation

and aggregation of the polyplexes, respectively. Therefore, higher branching resulted in higher gene transfer activity.

The other star polymers as a gene delivery vector are easily designed by iniferter-based photo-living-radical polymerization. The composition of polymer chains can be determined by the kind of monomers, and the molecular weight by the irradiation time. Therefore, in addition to allowing design of the basic skeletal structure, the composition and length of polymer chains can be optimized as schematically shown in (Fig. **4**). Changing the kind of monomers can control the composition of the polymer chains continuously or stepwise. To further increase the degree of branching, we will design the core molecules from benzene ring to naphthalene ring or combinations of benzene rings as multi-iniferters. Furthermore, formation of hyper branching structure by diverging of branching chains will be possible [34]. In the near future, the correlation between the three-dimensional structure in a star vector and the efficiency of gene expression will be clarified in detail.

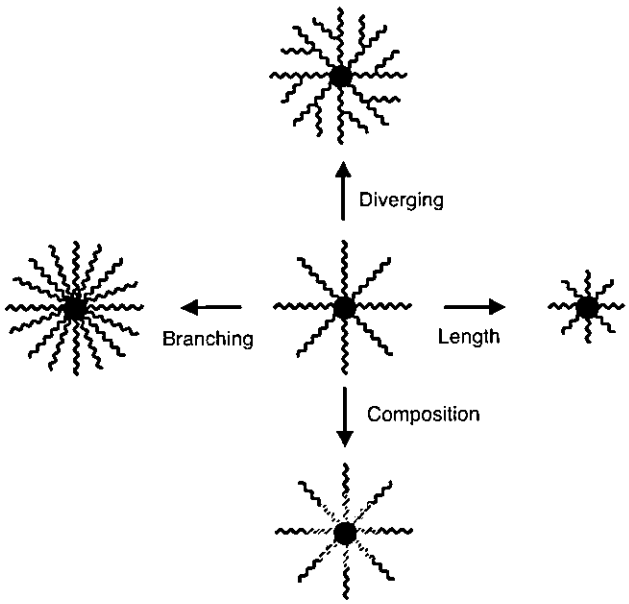

Fig. (4). Possibility in molecular design of various star polymers having different branching, diverging, chain length, or composition, which are based on iniferter-induced living radical polymerization.

ACKNOWLEDGEMENTS

This study was supported by "Research Grants for Advanced Medical Technology", "Human Genome, Tissue Engineering and Food Biotechnology", and "Aging and Health" from the Ministry of Health, Labor and Welfare of Japan, and by Grant-in-Aid for Scientific Research (B1-16390423) from the Ministry of Education, Science, Sports and Culture of Japan.

REFERENCES

[1] Felgner, P.; Barenholz, Y.; Behr, J.P.; Cheng, S.H.; Cullis, P.; Huang, L.; Jessee, F.J.; Seymour, L.; Szoka, F.; Thierry, A.R.; Wagner, E.; Wu, G. *Hum. Gene Ther.*, **1997**, *8*(5), 511-2.

[2] Niidome, T.; Huang, L. *Gene. Ther.*, **2002**, *9*(24), 1647-52.

[3] Thomas, M.; Klibanov, A.M. *Appl. Microbiol. Biotechnol.*, **2003**, *62*(1), 27-34.

[4] Gebhart, C.L.; Kabanov, A.K. *J. Control Release*, **2001**, *73*(2-3), 401-16.

[5] Nishikawa, M.; Huang, L. *Hum. Gene Ther.*, **2001**, *12*(8), 861-70.

[6] Kichise, T.; Taguchi, S.; Doi, Y. *Appl. Environ. Microbiol.*, **2002**, *68*(5), 2411-9.

[7] Zanta, M.A.; Boussif, O.; Adib, A.; Behr, J.P. *Bioconjug. Chem.*, **1997**, *8*(6), 839-944.

[8] Diebold, S.S.; Kursa, M.; Wagner, E.; Cotton, M.; Zenke, M. *J. Biol. Chem.*, **1999**, *274*(27), 19087-94.

[9] Kircheis, R.; Kichler, A.; Wallner, G.; Kursa, M.; Ogris, M.; Felzmann, T.; Buchberger, M.; Wagner, E. *Gene Ther.*, **1997**, *4*(5), 409-18.

[10] Wojda, U.; Miller, J.L. *J. Pharm. Sci.*, **2000**, *89*(5), 674-81.

[11] Li, S.; Tan, Y.; Viroonchatapan, E.; Pitt, B.R.; Huang, L. *Am. J. Physiol.*, **2000**, *278*(3), L504-11.

[12] Kurisawa, M.; Yokoyama, M.; Okano, T. *J. Control. Release*, **2000**, *69*(1), 127-37.

[13] Nagasaki, T.; Taniguchi, A.; Tamagaki, S. *Bioconjug. Chem.*, **2003**, *14*(3), 513-6.

[14] Nakayama, Y.; Umeda, M.; Uchida, K. unpublished data.

[15] Hui, S.W.; Stoicheva, N.; Zhao, Y.L. *Biophys. J.*, **1996**, *71*(2), 1123-30.

[16] Kuo, J.H.; Jan, M.S.; Sung, K.C. *Int. J. Pharm.*, **2003**, *257*(1-2), 75-84.

[17] Petersen, H.; Kunath, K.; Martin, A.L.; Stolnik, S.; Roberts, C.J.; Davies, M.C.; Kissel. T. *Biomacromolecules*, **2002**, *3*(5), 926-36.

[18] Zelikin, A.N.; Putnam, D.; Shastri, P.; Langer. R.; Izumrudov, V.A. *Bioconjug. Chem.*, **2002**, *13*(3), *548-53.*

[19] Kunath, K.; von Harpe, A.; Fischer, D.; Petersen, H.; Bickel, U.; Voigt, K.; Kissel, T. *J. Control. Release.*, **2003**, *89*(1), 113-25.

[20] Godbey, W.T.; Wu, K.K.; Mikos, A.G. *J. Biomed. Mater. Res.*; **1999**, *45*(3), 268-75.

[21] Fischer, D.; Bieber, T.; Li, Y.; Elsasser, H.P.; Kissel, T. *Pharm. Res.*, **1999**, *16*(8), 1273-79.

[22] Wightman, L.; Kircheis, R.; Rossler, V.; Carotta, S.; Ruzicka, R.; Kursa, M.; Wagner, E. *J. Gene Med.*, **2001**, *3*(4), 362-72.

[23] Van de Wetering, P., Moret, E.E.; Schuurmans-Nieuwenbroek, N.M.E.; van Streenbergen, M.J.; Hennik, W.E. *Bioconjug. Chem.* **1999**, *10*(4), 589-97.

[24] Tang, M.X.; Szoka, F.C. *Gene Ther.*, **1997**, *4*(8), 823-32.

[25] Otsu, T.; Yoshida, M, *Makromol. Chem. Rapid Commun.*, **1982**, *3*, 127-32.

[26] Otsu, T.; Yoshida, M.; Tazaki, T. *Makromol. Chem., Rapid Commun.*, **1982**, *3*, 133-40.

[27] Otsu, T.; Matsunaga, T.; Doi, T.; Matsumoto, A.; *Eur. Polym. J.*, **1995**, *31*, 67-78.

[28] Otsu, T.; Matsumoto, *Advances in Polymer Science*, **1998**, *136*, 75-137.

[29] Matyjaszewski, K. Ed. *Controlled radical polymerization.* ACS Symposium Series 685 American Chemical Society: Washington, DC, **1998**.

[30] Sawamoto, M.; Kamigaito, M. In *Polymer Synthesis; Materials Science and Technology Series*; VCH-Wiley: Weinheim, **1998**; Chapter 1.

[31] Nakayama, Y.; Matsuda, T. *Macromolecules*, **1996**, *29*(27), 8622-30.

[32] Nakayama, Y.; Matsuda, T. *Langmuir*, **1999**, *15*(17), 5560-66.

[33] Higashi, J.; Nakayama, Y.; Marchant, R.E.; Matsuda, T. *Langmuir*, **1999**, *15*(6), 2080-8.

[34] Nakayama, Y.; Sudo, M.; Uchida, K.; Matsuda, T. *Langmuir*, **2002**, *18*(7), 2601-6.

[35] Ferrari, S.; Moro, E.; Pettenazzo, A.; Behr, J.P.; Zacchello, F.; Scarpa, M. *Gene Ther.*, **1997**, *4*(10), 1100-6.

[36] Coll, J.L.; Chollet, P.; Brambilla, E.; Desplangues, D.; Behr, J.P.; Favrot, M. *Hum. Gene Ther.*, **1999**, *10*(10), 1659-66.

[37] Boussif, O.; Zanta, M.A.; Behr, J.P. *Gene Ther.*, **1996**, *3*(12), 1074-80.

[38] Sonawane, N.D.; Szoka, F.C. Jr.; Verkman, A.S. *J. Biol. Chem.*, **2003**, *278*(45), 44826-31.

Received: July 01, 2004 Accepted: August 03, 2004

Disruption of Autosomal Recessive Hypercholesterolemia Gene Shows Different Phenotype In Vitro and In Vivo

Mariko Harada-Shiba, Atsuko Takagi, Kousuke Marutsuka, Sayaka Moriguchi, Hiroaki Yagyu, Shun Ishibashi, Yujiro Asada, Shinji Yokoyama

Abstract—We previously characterized the patients with autosomal recessive hypercholesterolemia (ARH) as having severe hypercholesterolemia and retarded plasma low-density lipoprotein (LDL) clearance despite normal LDL receptor (LDLR) function in their cultured fibroblasts, and we identified a mutation in the *ARH* locus in these patients. ARH protein is an adaptor protein of the LDL and reportedly modulates its internalization. We developed ARH knockout mice ($ARH^{-/-}$) to study the function of this protein. Plasma total cholesterol level was higher in $ARH^{-/-}$ mice than that in wild-type mice ($ARH^{+/+}$), being attributed to a 6-fold increase of LDL, whereas plasma lipoprotein was normal in the heterozygotes ($ARH^{+/-}$). Clearance of ^{125}I-LDL from plasma was retarded in $ARH^{-/-}$ mice, as much as that found in $LDLR^{-/-}$ mice. Fluorescence activity of the intravenously injected 1,1′-dioctadecyl-3,3,3′,3′-tetramethylindocarbocyanine perchlorate (DiI)-LDL was recovered in the cytosol of the hepatocytes of $ARH^{+/+}$ mice, but not in those of $ARH^{-/-}$ or $LDLR^{-/-}$ mice. Also, less radioactivity was recovered in the liver of $ARH^{-/-}$ or $LDLR^{-/-}$ mice when [^{3}H]cholesteryl oleyl ether (CE)-labeled LDL was injected. In contrast, uptakes of [^{3}H]CE-labeled LDL, ^{125}I-LDL, and DiI-LDL were all normal or slightly subnormal when the $ARH^{-/-}$ hepatocytes were cultured. We thus concluded that the function of the hepatic LDLR is impaired in the $ARH^{-/-}$ mice in vivo, despite its normal function in vitro. These findings were consistent with the observations with the ARH homozygous patients and suggested that certain cellular environmental factors modulate the requirement of ARH for the LDLR function. (***Circ Res.* 2004;95:945-952.**)

Key Words: autosomal recessive hypercholesterolemia ■ knockout mouse ■ low-density lipoprotein receptor ■ primary cultured hepatocytes ■ OmniBank

Hereditary hypercholesterolemia was first characterized by Khachadurian and Kuthman in 1973[1] as severe hypercholesterolemia with cutaneous and tendon xanthomas and premature atherosclerosis. They proposed two categories, autosomal dominant and recessive.[1] Hypercholesterolemia with autosomal dominant inheritance was termed familial hypercholesterolemia. Studies of familial hypercholesterolemia led to the discovery of low-density lipoprotein receptor (LDLR) and identification of its genetic dysfunction as the cause of this disease. The LDLR is now known to play a key role in the internalization of LDL into the cell and in the regulation of plasma LDL concentrations.[2,3] However, hypercholesterolemia with autosomal recessive inheritance had never been fully characterized until we first reported this disease.[4,5] In these articles, we described siblings with severe hypercholesterolemia, exhibiting huge xanthomas and premature atherosclerosis despite normal LDLR activity in their cultured fibroblasts.

In 2001, Garcia et al[6] mapped the *ARH* locus to chromosome 1p35 using six families of autosomal recessive hypercholesterolemia (ARH). They identified six mutations of the gene encoding a putative LDLR adaptor protein in these ARH families. We showed that an insertion mutation in the *ARH* gene of the Japanese siblings described causes an early stop codon.[7]

ARH protein has an N-terminal phosphotyrosine-binding (PTB) domain.[6] The PTB domain is found in several adaptor proteins, such as Disabled-2 and numb, and binds to an NPXY sequence in the cytoplasmic tails of cell surface receptors to modulate their internalization. Recently, the PTB domain of ARH protein was shown by the pull-down technique to bind to the FDNPVY sequence of LDLR.[8] ARH protein was also reported to interact with clathrin and is thought to function as an adaptor protein that couples LDLR to the endocytic machinery.[8]

What is unique about the patients with ARH is the apparent inconsistency of the LDLR functions between in vitro and in

Original received October 24, 2003; resubmission received June 10, 2004; revised resubmission received September 13, 2004; accepted September 24, 2004.

From the Department of Bioscience (M.H.-S.), Department of Pharmacology (A.T.), National Cardiovascular Center Research Institute, Osaka; First Department of Pathology (K.M., S.M., Y.A.), Miyazaki Medical College, Miyazaki; Division of Endocrinology and Metabolism (H.Y., S.I.), Jichi Medical School, Kawachi-gun, Tochigi; Department of Biochemistry, Cell Biology, and Metabolism (S.Y.), Nagoya City University Graduate School of Medical Sciences, Mizuho-cho, Nagoya, Aichi, Japan.

Correspondence to Mariko Harada-Shiba, Department of Bioscience, National Cardiovascular Center Research Institute, Fujishiro-dai, Suita, Osaka 565-8565, Japan. E-mail mshiba@ri.ncvc.go.jp

Circulation Research is available at http://www.circresaha.org DOI: 10.1161/01.RES.0000146946.78540.46

vivo. In ARH patients, clearance of ^{125}I-LDL from plasma is delayed to the same extent as that found among homozygous familial hypercholesterolemia, whereas LDL binding, internalization, and degradation are normal or subnormal in their cultured fibroblasts.[9–11] However, a defect in LDLR internalization was observed in Epstein-Barr virus lymphocytes from ARH patients.[12] LDLR activity in these mutant cells could be restored by retrovirus-mediated expression of normal ARH.[13] The results indicated that lymphocytes require ARH for normal functioning of the LDLR even in vitro, whereas fibroblasts express the normal LDLR functions without ARH, at least in vitro. Because ARH patients have delayed clearance of LDL, the LDLR requires ARH for its functions, at least in the liver in vivo. Jones et al[14] reported that ARH-deficient mice have delayed catabolism of LDL, higher LDL cholesterol levels, and greater immunodetectable LDLR on the sinusoidal surface of hepatocytes.

In the present study, we characterized *ARH*-deficient mice to study the functions of ARH. *ARH*$^{-/-}$ mice showed a higher level of plasma LDL cholesterol than wild-type mice, whereas *ARH*$^{+/-}$ mice did not show hypercholesterolemia, being consistent with clinical manifestation of the human ARH patients.[5,7] The clearance of ^{125}I-LDL was delayed, and hepatic uptake of 1,1′-dioctadecyl-3,3,3′,3′-tetramethylindocarbocyanine perchlorate (DiI)-LDL and of [^{3}H]cholesteryl oleyl ether-labeled LDL (^{3}H-CE-LDL) was decreased in *ARH*$^{-/-}$ mice. However, primary cultured hepatocytes of *ARH*$^{-/-}$ mice had normal functions to internalize ^{3}H-CE-LDL, ^{125}I-LDL, and DiI-LDL. Thus, the results indicate that the cellular environment modulates the regulation of LDLR function by ARH protein.

Materials and Methods

General Procedure

Plasma lipoproteins were analyzed by high-performance liquid chromatography using molecular sieve columns (Skylight Biotech, Inc).[15] Cholesterol and triglycerides were measured using enzyme assay kits (Wako, Tokyo, Japan). Na^{125}I (37 GBq/mL) and [1α,2α(*n*)-^{3}H]cholesteryl oleyl ether (^{3}H-CE) (1.63 TBq/mmol) were purchased from Amersham (Buckinghamshire, UK). LDL was isolated by sequential ultracentrifugation in a density range of 1.019<density<1.064 from pooled plasma of apolipoprotein E knockout mice (Jackson Laboratory, Bar Harbor, Me) or normal human volunteers after overnight fasting. Human lipoprotein-deficient serum (LPDS) (density>1.215 g/mL) was prepared by ultracentrifugation.

Generation of Knockout Mouse

To generate *ARH* knockout mice, mutations were created by insertional mutagenesis using the gene trap vectors developed by Lexicon Genetics Incorporated (Woodlands, Tex), based on retroviral-based gene trap technology previously reported.[16] OmniBank Sequence Tag 149604 corresponded to the insertion mutation in the third intron of *ARH* gene in mouse chromosome 4 (Figure 1A). The line was obtained from Lexicon Genetics Incorporated. All experiments were performed with the F2-generation or F3-generation descendants, which were backcrossed with the C57Bl/6. LDLR knockout mice (*LDLR*$^{-/-}$) were generated as previously described,[17] which were backcrossed to C57Bl/6 mice, and were used for the study.

Southern Blot Analysis

Southern blot analysis was performed after digestion of the DNA prepared from liver with *Apa*I. ^{32}P-labeled polymerase chain reaction products (239 bp) amplified from portions of exon 3 and intron 3 of the mouse *ARH* gene with primers 5′-ATCATCCTGACCGACAGCCT-3′ and 5′-GGCACAACATAACCGACCTA-3′ or neo gene fragment (850 bp) derived from pBS64neo (Lexicon Genetics Inc) as probes according to the standard procedure.[18]

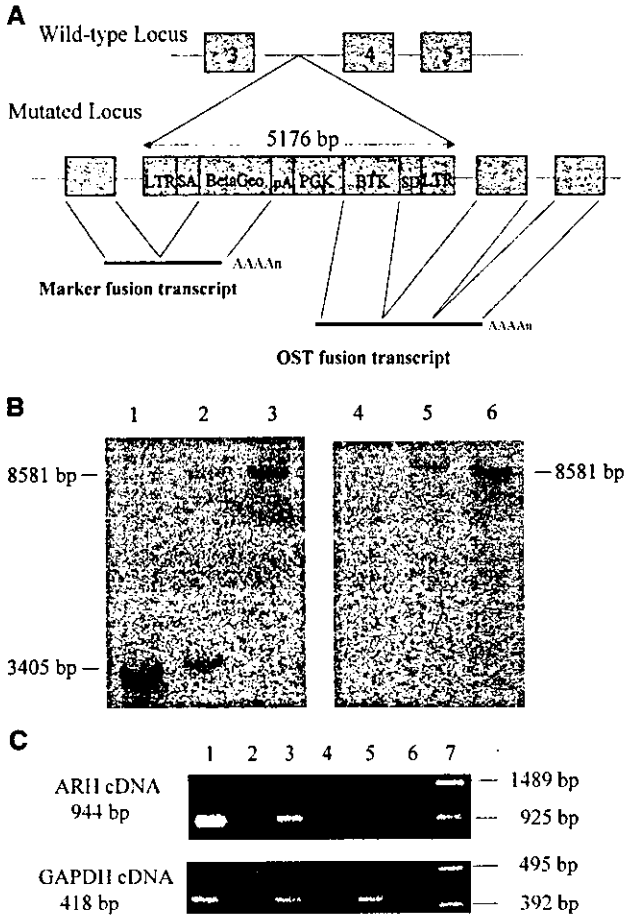

Figure 1. A, Strategy for insertional mutagenesis of the *ARH* locus in the mouse genome. The gene trap vector contains a promoterless splice acceptor sequence (SA) and BetaGeo, which create marker fusion transcripts. The vector also contains a long terminal repeat (LTR), a phosphoglycerate kinase-1 promoter (PGK), Bruton tyrosine kinase (BTK), and a splice donor sequence (SD). OmniBank Sequence Tag 149604 has an insertion of the vector in the third intron of *ARH* gene. B, Southern blot analysis of liver DNA. DNA was digested with *Apa*I and hybridized with a probe comprising portions of the mouse *ARH* gene containing exon 3 and intron 3 (lanes 1 to 3) or neo gene (lanes 4 to 6). Lanes 1 and 4, *ARH*$^{+/+}$; lanes 2 and 5, *ARH*$^{+/-}$; lanes 3 and 6, *ARH*$^{-/-}$. C, Reverse-transcription polymerase chain reaction of ARH and GAPDH mRNA. Lane 1 and 2, *ARH*$^{+/+}$; 3 and 4, *ARH*$^{+/-}$; 5 and 6, *ARH*$^{-/-}$. Lane 1, 3, and 5 are reverse-transcription plus; 2, 4, and 6 are reverse-transcription minus. Lane 7 shows size markers, lambda DNA digested with *Sty*1 for ARH, and phiX174 DNA digested with *Hin*cII for GAPDH.

Reverse-Transcription Polymerase Chain Reaction

Total RNA was isolated from the liver of wild-type, heterozygous, and homozygous mice using the acid guanidium thiocyanate-phenol-chloroform method, as described.[19]

^{125}I-LDL Turnover Study

Mouse LDL was iodinated with ^{125}I by the iodine monochloride method[20] to give a specific activity of ^{125}I-LDL >200 cpm/ng